

Stony Brook University



OFFICIAL COPY

The official electronic file of this thesis or dissertation is maintained by the University Libraries on behalf of The Graduate School at Stony Brook University.

© All Rights Reserved by Author.

Synthesis of a Fluorescent Sensor for Calcium Measurement in Marine Sediments

A Thesis Presented

by

Jingyu Huang

to

The Graduate School

in Partial Fulfillment of the

Requirements

for the Degree of

Master of Science

in

Chemistry

Stony Brook University

August 2013

Stony Brook University

The Graduate School

Jingyu Huang

We, the thesis committee for the above candidate for the
Master of Science degree, hereby recommend
acceptance of this thesis.

**Dale G. Drueckhammer – Thesis Advisor
Professor, Department of Chemistry**

**Nancy S. Goroff – Chair
Associate Professor, Department of Chemistry**

**Stephen A. Koch – Third Member
Professor, Department of Chemistry**

This thesis is accepted by the Graduate School

Charles Taber
Interim Dean of the Graduate School

Abstract of the Thesis

Synthesis of a Fluorescent Sensor for Calcium Measurement in Marine Sediments

by

Jingyu Huang

Master of Science

in

Chemistry

Stony Brook University

2013

Ocean acidification has been shown to endanger shelled marine organisms, since increased CO₂ intake by oceans will decrease pH of seawater and enhance Ca²⁺ dissolution from shell skeletons. Determination of Ca²⁺ concentration in the marine environment would not only help to provide information about local calcium ion distribution and activities, but also provide a sketch of the living condition of shelled marine organisms. A number of optical sensors for calcium ion detection have been developed. However, these detectors were mostly designed for intracellular detections or relatively low ion concentration conditions (10⁻⁶ to 10⁻⁸ M) and have high calcium affinity, which is not suitable to apply in a marine environment where calcium concentration is much higher (~10mM). The objective of this project is to develop a fluorescence-based calcium sensor with low calcium affinity for calcium distribution imaging in marine environments. The synthesis of this sensor is the first step towards the development of an optical instrument for direct *in situ*, non-destructive and high-resolution two dimensional imaging of Ca²⁺. The experimental approach involves the coupling of a fluorophore with a calcium binding ligand. When binding to calcium ions, the fluorescence of the sensor will increase and hence shows

correlation to calcium concentration in the sample. Further steps include verification of the coupling product, examination of the calcium ion binding ability, and possibly the application in artificial marine settings.

Table of Contents

Chapters

1. Effects on Increasing Atmospheric CO ₂ on Calcium Distribution in Marine Environments and Organisms	1
1-1. Overview of Calcium in Seawater	1
1-2. Interaction between Atmospheric Carbon Dioxide and Calcium Carbonate System in Oceans	2
1-3. Impact of Increased Atmospheric Carbon Dioxide on Marine CaCO ₃ - Secreting Organisms	8
2. Design and Synthesis of a Calcium Sensor for Use in Marine Environments	11
2-1. Introduction	11
2-2. Overview of Synthetic Route.....	14
2-3. Results and Discussion	16
2-3-1. Synthesis of Ca ²⁺ Binding Moiety.....	16
2-3-2. Synthesis of the Fluorophore.....	23
2-3-3. Coupling of the Binding amine and the Acid Chloride derivatives of the Fluorophore.....	27
3. Experimental Design and Methods	37
References.....	45
Appendices.....	49

List of Figures

Figure 1. Fluorescent signaling from the sensor upon binding with a calcium ion.	11
Figure 2. Synthetic design involves the coupling of fluorophore (6) with the calcium binding amine (3) in dichloromethane. Deprotection of the two acetate groups yields the final product.	13
Figure 3. Formation Mechanism of Nitrosyl Cation in Acetic Acid.....	20
Figure 4. Interference coupling of the residual acetic acid or oxalyl chloride with the Ca ²⁺ binding amine (3).....	30
Figure 5. Polar solvent systems tried for separation of purified fractions with high polarity.	32
Figure 6. Compound (1), diethyl 2,2'-((2-methoxyphenyl)azanediyl) diacetate.	37
Figure 7. Compound (2), diethyl 2,2'-((2-methoxy-4-nitrosophenyl)azanediyl)diacetate.	38
Figure 8. Compound (3), diethyl 2,2'-((4-amino-2-methoxyphenyl)azanediyl)diacetate.	39
Figure 9. Compound (4a, 4b), 2',7'-Dichloro-5(6)- carboxylfluorescein.	40
Figure 10. Compound (5a, 5b), 3',6'-diacetyl-2',7'-dichloro-6-carboxyfluorescein pyridine salt and 3',6'-diacetyl-2',7'-dichloro-5-carboxyfluorescein	41
Figure 11. Compound (6a, 6b), 2',7'-dichloro-5(6)-(chlorocarbonyl)-3-oxo-3H-spiro[isobenzofuran-1,9'-xanthene]-3',6'-diyl diacetate.	42
Figure 12. Designed protected sensor structure, diethyl 2,2'-((4-(3',6'-diacetoxy-2',7'-dichloro-3-oxo-3H-spiro[isobenzofuran-1,9'-xanthene]-6-ylcarboxamido)-2-methoxyphenyl)azanediyl)diacetate.....	43
Figure 13. Designed deprotection of cruder sensor.....	44

List of Schemes

Scheme 1. The complete synthetic route includes three main sessions: synthesis of the Ca ²⁺ binding amine; synthesis of the fluorophore; and the coupling of the binding amine and the fluorophore.....	15
Scheme 2. Detailed scheme of synthesizing Ca ²⁺ amine: alkylation of o-anisidine; nitrosation; and reduction of the nitroso-compound (2).	16
Scheme 3. Step 1: Double alkylation of o-anisidine with ethyl bromoacetate to yield (1).	17
Scheme 4. Step 2: Nitrosation of (1) to yield (2) in acetic acid.....	18
Scheme 5. Step Three: Reduction of (2) to an arylamine (3) ammonium formate on catalysis of Pd/ C...	21
Scheme 6. Detailed scheme of synthesizing the carboxyfluorescein: formation of chlorinated derivatives of 5(6) –carboxyfluorescein (4a, 4b); protection of the carboxyfluorescein; conversion of the acid- form isomer to the acid chloride form.	23
Scheme 7. Step Four: Formation of chlorinated derivatives of 5(6) –carboxyfluorescein (4a, 4b).	24
Scheme 8. Step Five: Protection of the carboxyfluorescein by acetic anhydride.....	24
Scheme 9. Step Six: Conversion of carboxylfluorescein into an acid chloride form.	26
Scheme 10. Designed coupling of the amine and fluorophore and deprotection of resulted product.	27
Scheme 11. Coupling from isomer (5a).....	28

List of Tables

Table 1. Examples of marine species/ organisms affected by ocean acidification. ⁵	10
Table 2. Information of Second Attempt to prepare Diethyl 2,2'-((2-methoxy-4-nitrosophenyl)azanediyl)diacetate (2).....	20
Table 3. Summary of coupling reaction attempts.	35

List of Abbreviations

cALK: carbon alkalinity

CTH: catalytic transfer hydrogenation
(AF- CTH: ammonium formate- catalytic transfer hydrogenation)

DIC: dissolved inorganic carbon

DMF: N,N-Dimethylmethanamide

EA: ethyl acetate

JGOFS: Joint Global Ocean Flux Study

OA: ocean acidification

ppmv: parts per million by volume

TA: total alkalinity

TCO₂: total carbonate

TEA: triethylamine

WOCE: World Ocean Circulation Experiment

Chapter One

Effects on Increasing Atmospheric CO₂ on Calcium Distribution in Marine Environments and Organisms

1-1. Overview of Calcium in Seawater

Calcium is an important element in the oceans. While most of the element appears in the ionic form Ca²⁺ in seawater, a fraction of calcium ions (10-15%) combine with other free ions present to form precipitates or ion pairs, accounting for 1.2% by weight of the sea salt species.^{1,2} Many of these combinations, however, either are short-lived (e.g. CaSO₄) or have little effect on the marine calcium system overall due to lower Ca²⁺ affinity to anions compared to Mg²⁺ (e.g. CaF⁺). The most stable and important form of calcium in marine environment is calcium carbonate CaCO₃, which is a major component of the skeletons and shells of many corals and other organisms, as well as deep sea deposit.^{2,3,4} Most concerns regarding marine calcium or substantially the CaCO₃ system in the oceans arise from increasingly serious ocean acidification. This can lead to the dissolution of these calcium carbonate structures and hence possible changes in marine biodiversity and other ecosystem consequences, as well as imbalance of seawater chemistry.^{4,5}

1-2. Interaction between Atmospheric Carbon Dioxide and Calcium Carbonate System in Oceans

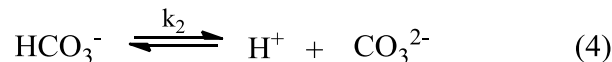
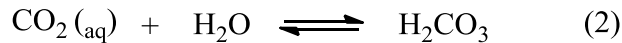
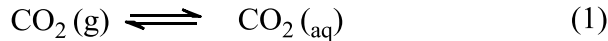
Ocean Acidification is now a well-known term describing the decrease in seawater pH and alteration of seawater chemistry by excessive anthropogenic carbon dioxide output. As a major sink taking up carbon dioxide from the atmosphere, the oceans absorb approximately one-third of the anthropogenic CO₂ generated between 1800 and 1994, which equals an oceanic uptake of 118 ± 19 Pg C (1 Pg C = 10^{15} g of C) of anthropogenic carbon.^{3,7} Without the ocean sinks, the atmospheric CO₂ concentration was expected to be 55% higher than the observed change from 280 ppmv to 380 ppmv within the past 200 years. Such a reduced amount of CO₂ in the atmosphere however, has lowered the average seawater pH by 0.1 unit which is equally an increase of about 30% in [H⁺].^{5, 6, 7} At a current concentration of 380 ppmv, atmospheric CO₂ concentration is rising approximately 0.5% year⁻¹ which is unprecedented in the past 650 000 years. Under the intergovernmental panel on climate change emission scenarios and general circulation models, CO₂ concentration will reach 800 ppmv by the end of this century, and the average seawater pH will decrease another 0.3-0.4 units. Moreover, CO₂ concentration is expected to rise to 2000 ppmv over the next two centuries.^{3,5,7,8}

The specific mechanism of how the anthropogenic CO₂ is taken up, conveyed, and deposited by the ocean sinks is currently not well-known,⁷ even though there is little uncertainty that ocean acidification is caused by the rising carbon dioxide concentration in the atmosphere. Investigation of carbon dioxide in seawater dates back to the beginning of the 19th century and became more intense since the 1960s. The increased interest in CO₂ measurement in marine environments in the mid-twentieth century, however, was to collect data for simple analysis. The potential impact that aqueous carbon dioxide has on marine biota was neglected by researchers at

that time since calcium carbonate (calcite/ aragonite) was expected to remain supersaturated in surface seawater, even though they were knowledgeable of an equilibrium relationship between the oceanic and atmospheric CO₂.^{6,7} Relatively comprehensive studies regarding interaction of increased dissolved carbon dioxide and the carbon (CaCO₃) system in the oceans were conducted in a more precise degree around the 1990s, including projects such as World Ocean Circulation Experiment (WOCE) and the Joint Global Ocean Flux Study (JGOFS).⁷ Studies have shown that approximately 30% of the anthropogenic CO₂ is held in seawater no deeper than two hundred meters, and about one half remains within the upper four hundred meters. Such absorbed carbon dioxide has reduced the global average seawater pH from about 8.21 in pre-industrial period to the present value of 8.1, and has lowered the calcium carbonate saturation state in surface seawater.^{3,5,6,7} Nevertheless, the long-term impact of increased atmospheric and hence dissolved CO₂ in oceans has on the marine ecosystem is not yet known in detail. The reasons are mainly 1) comprehensive examination of carbon dioxide system was developed relatively lately, and 2) studies regarding the carbon (CaCO₃) system in marine environment are mostly limited to certain areas (e.g tropical and coastal regions) and certain species (e.g coral reefs and coccolithophores). A great deal of effort is therefore still required in the field to provide a complete projection of both the atmospheric CO₂ and marine carbon system.^{3,5,6,7}

Research aiming to investigate the impact of carbon dioxide on CaCO₃ structures/ calcifying organisms mainly focus on the study of dissolved inorganic carbon (DIC) distribution and total salinity.³ According to Millero et al.,⁹ four parameters are actually involved for the characterization of the carbon system: pH, fugacity of carbon dioxide (f_{CO_2}), total carbonate (TCO₂), and total alkalinity (TA). Two of the four are usually measured and sufficient for carbon

index. The others can be obtained through thermodynamic equations. In such a sense, dissolved inorganic carbon (DIC) mentioned above which is widely applied later in most literature, represents the homologous parameter as TCO₂ in Millero's notion.^{3,5,7} Major components of dissolved inorganic carbon are bicarbonate ions (HCO₃⁻), carbonate ions (CO₃²⁻), and dissolved CO₂ (CO_{2(aq)}). When CO₂ dissolves in seawater (CO_{2(aq)}), it combines with a water molecule to form carbonic acid (H₂CO₃), which is a weak acid and therefore the two species are in equilibrium and difficult to distinguish. In fact, the sum of CO_{2(aq)} and H₂CO₃ is usually applied as one parameter in studies.⁹ H₂CO₃ then ionizes twice into two hydrogen ions (H⁺), a bicarbonate ion (HCO₃⁻), and a carbonate ion (CO₃²⁻) (Eq. 1-4). However, the second ionization is less efficient than the previous since the first proton in carbonic acid is more acidic (pKa₁ < pKa₂).⁹ Even though all of these reactions occur reversibly in seawater, the net effect of dissolution of CO₂ in seawater is the consumption of carbonate ions (conversion to bicarbonate ions) in the oceans. At a current pH of 8.1, concentrations of DIC are 90% HCO₃⁻, 9% CO₃²⁻, and 1% (CO_{2(aq)}). Changes in these concentrations within the last 200 years (comparing to pre-industrial period) confirm the impact resulted from anthropogenic CO₂ input: [CO₃²⁻] has decreased by 2% while [CO_{2(aq)}] has increased by 0.5%.^{5,6}



The total alkalinity is calculated as the difference between cations (e.g. Na^+ , Ca^{2+}) and anions (e.g. Cl^- , F^-) whose concentrations are relatively stable in seawater. Namely, total alkalinity represents the ionic balance and the capacity of seawater to accept acidic species. When considering the carbon system, TA is simplified to be the carbonate alkalinity (cALK) which is the sum of charged components that only correspond to carbonate species. Since the single-charged HCO_3^- binds only one proton, the proton capacity of CO_3^{2-} is double of that of the bicarbonate ion.^{4,9}

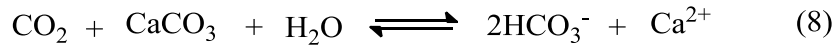
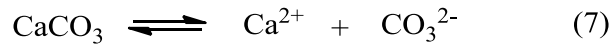
$$\text{cALK} = [\text{HCO}_3^-] + 2 [\text{CO}_3^{2-}] \quad (5)$$

As the absorption of atmospheric carbon dioxide decreases the concentration of carbonate ions in seawater, it directly affects marine calcifying organisms including corals, mollusks, pelagic planktons and others, which form shells and skeletons (CaCO_3) relying on CO_3^{2-} availability.^{5,6} Whether the carbonates dissolve or precipitate in seawater depends on the CaCO_3 saturation state (Ω) of the water body. Ω is proportional to the ionic product of calcium and carbonate concentrations:

$$\Omega = [\text{Ca}^{2+}] [\text{CO}_3^{2-}] / K_{\text{sp}}^* \quad (6)$$

K_{sp}^* is the apparent solubility product of CaCO_3 , which depends on ambient conditions such as temperature, salinity, pressure, and the specific mineral phase.⁶ Aragonite and calcite are the two main forms of CaCO_3 that associate with marine biota and therefore Ω is usually referred to Ω_{arag} and Ω_{cal} . Concentration of calcium ions is proportional to salinity of seawater. Since $[\text{Ca}^{2+}]$ is

quite stable (variation of Ca/ salinity ratio is usually less than 1.5%), Ω is mainly determined by $[\text{CO}_3^{2-}]$ which can be obtained from dissolved inorganic carbon and total alkalinity.^{3,5,6} The saturation state represents an index for calcium carbonate condition in the examined ocean sample. Formation of CaCO_3 (shell/ skeleton structures) are more likely to occur when Ω is greater than 1. When Ω is less than 1, implying a deficiency of Ca^{2+} and CO_3^{2-} , the reaction equilibrium shifts to favor the formation of these ions (dissolution of shells/ skeletons) (Eq. 7).⁶ The net chemical equation of the dissolution of CaCO_3 structures has resulted from the absorption of atmospheric CO_2 in the oceans is therefore derived as shown in Eq. 8.



Since the pre-industrial period, oceans around the world have shown either shoaling (upward migration) of the saturation horizon with respect to calcite or aragonite (below which the particle begins to dissolve),⁴ or expansion of the unsaturation zone due to ocean acidification. Solubility of CaCO_3 positively correlates to pressure but has an inverse correlation with respect to temperature. In the vertical scheme of the ocean, CaCO_3 state transfers from saturated to under saturated from the surface to deep sea water, i.e., dissolution of oceanic CaCO_3 is expected to primarily occur under deep sea.^{3,4} And in a global scale, the highest CaCO_3 saturation state is found in warm waters around tropics and subtropical areas; while lower CaCO_3 saturation state or under saturation conditions are usually in colder high-latitude regions.^{5,6} As CO_2 enters the ocean by gas exchange above the air-sea interface, the dissolved CO_2 remains in the upper level dissolving the CaCO_3 deposits, and therefore causes the saturation horizon ($\Omega = 1$) to shoal.^{6,7}

According to Feely et al.,³ atmospheric CO₂ together with biological processes have shoaled the aragonite saturation depth in the Arabian Sea and Bay of Bengal (north of 30 °S in the Indian Ocean) 100 to 200 m shallower compared to two hundred years ago. The calcite saturation horizon north of 20 °N in the Pacific Ocean has also been shoaled by greater CO₂ pressure 40 to 100 m upward, and about 80 to 100 m in the east Atlantic.³

1-3. Impact of Increased Atmospheric Carbon Dioxide on Marine CaCO₃- Secreting Organisms

Calcium carbonate- secreting organisms include many species across the marine animal phyla and many of them are common features that live within shallow seawater/sediment area (e.g. oysters) well- known by human.⁵ Researches have shown that these calcifying organisms will be facing great life threat due to the shoaling of CaCO₃ saturation horizon. In the study of Green et al.(2004),¹⁰ the hard-shell clam *Mercenaria mercenaria* was observed to suffer complete dissolution of the CaCO₃ shell within two weeks when placed in an under- saturation surrounding (with respect to aragonite, $\Omega_{\text{arag}} \sim 0.3$), which is a typical level for near-shore surface sediment rich with organic components. Live *Clio pyramidata* from the Subarctic Pacific were found to undergo shell dissolution within 48 hours when exposed to an aragonite under saturation environment, which is the projected level for Southern Ocean surfaces in the year 2100 based on the IS92a “business-as-usual” scenario.⁵

Impacts that shoaling of the CaCO₃ saturation horizon and the resulting decrease in calcification have on the marine ecosystem include change in geographic distribution of species, regional species composition, and marine foodweb structures, etc.^{3,5,11} Among the many affected species, *Eutecosomatous pteropods* are relatively well-studied. These pteropods are found in polar and subpolar regions, serving as the predators for various fish species and the popular prey for several species including pink salmon.⁶ Calcifying organisms like *Eutecosomatous pteropods* will have to adjust to fit in a more corrosive and limited habitat (lower pH and shoaling of CaCO₃ saturation horizon), or to migrate to calcium carbonate saturated but warmer waters in order to maintain survival. Shifting the habitat however will be challenging and probably limited for these pteropods due to extreme change in temperature.⁵ While calcifying

organisms are positioned in an disadvantaged situation, non- calcifying creatures will benefit and therefore probably dominate,¹² leading to a loss in balance of the regional species scheme which has established over a long evolutionary period. Moreover, again taking *Euthecosomatous pteropods* for example, since they account for more than 60% of the diet of pink salmon (in North Pacific), failure of the pteropods survival will have a severe effect on the production and well-being of the commercially popular fish.^{5,6} This will then lead to negative impacts on human economic activity (fisheries) and even food availability. In addition to the high- latitude pteropods, near-shore bivalves such as mussels and oysters are also threatened by decreased calcium carbonate saturation.⁵ Although specific species studies (e.g. corals and *Euthecosomatous pteropods*) have provided researchers with information about excessive atmospheric CO₂ impact on marine calcifying organisms, the long-term effects on the marine ecosystem are still not well-known due to the lack of information/ data and the complicated connections among marine organisms.^{5,6} In other words, scientists are currently still not able to make a conclusive prediction regarding the changes in marine environments under rising CO₂ pressure. A great amount of study is urgently required from multiple aspects to provide a comprehensive understanding of the consequences brought by ocean acidification. Table 1 listed additional marine organisms summarized as by Farby et al. that are affected by ocean acidification.⁵

Species	Description	CO₂ Condition	Sensitivity
<i>Mytilus edulis</i>	Mussel	pCO ₂ 740 ppmv	25% decrease in calcification rate
<i>Crassostrea gigas</i>	Oyster	pCO ₂ 740 ppmv 10%	decrease in calcification rate
<i>Placopecten magellanicus</i>	Giant scallop	pH < 8.0	Decrease in fertilization and embryo development
<i>Hemicentrotus</i>	Sea urchin	~ 500 – 10 000 ppmv	Decreased fertilization rates, impacts larval development
<i>Paralichthys olivaceus</i>	Japanese flounder	5% CO ₂ , ~ 50 000 ppmv	100% mortality within 48 h
<i>Pagrus major</i>	Red sea bream	5% CO ₂ , ~ 50 000 ppmv	>60% larval mortality after 24 h
<i>Seriola quinqueradiata</i>	Yellowtail/ amberjack	5% CO ₂ , 50 000 ppmv	Reduced cardiac output; 100% mortality after 8 h
<i>Euthynnus affinis</i>	Eastern little tuna	15% CO ₂ , ~ 150 000 ppmv	100% mortality of eggs after 24 h

Table 1. Examples of marine species/ organisms affected by ocean acidification.⁵

Chapter Two

Design and Synthesis of a Calcium Sensor for Use in Marine Environments

2-1. Introduction

Many on-going researches developed nowadays are performed in the laboratory in an artificial seawater system and they focus on observing how the examined organisms respond biologically to the specific settings.^{5,13} Few studies aim to analyze changes in marine calcium carbonate chemistry, and they mostly measure the concentration of carbonate ions (from total alkalinity and dissolved inorganic carbon).^{3,11} Though established models represent decent measurement of current CO_3^{2-} levels and good projections for the future, they do not provide information regarding Ca^{2+} . The objective of this project is to synthesize a calcium indicator, which is capable to bind with free Ca^{2+} in marine sediment and generate fluorescent signal upon the attachment (Fig. 1). The detection of Ca^{2+} concentration in marine sediment not only provides a second direction (in addition to the investigation of CO_3^{2-}) to understand the impact that ocean acidification has on calcifying organisms (especially those living near-shore), but also provides information about the biological activity of the organisms under the specific target environment (for a certain pH, etc).¹⁴

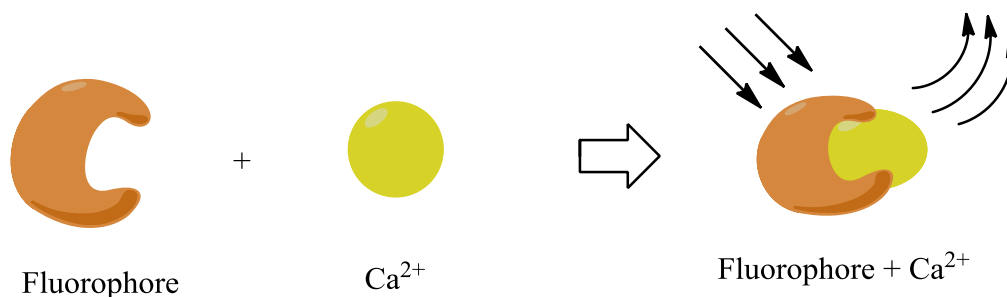


Figure 1. Fluorescent signaling from the sensor upon binding with a calcium ion.

Ca^{2+} signaling has been a popular topic in research since decades ago.¹⁵ However, the original and even present interest is mainly to measure intracellular calcium levels due to increasing discovery of the close connection between calcium condition and a series of biological activities such as autophagy, and hence human health.^{15,16} Many tracing molecules have been designed and used for calcium detection in physiological environments.¹⁵⁻¹⁹ Yet none has been designed for the detection of calcium under other conditions such as in seawater, probably due to lack of research interest in oceanic alkaline chemistry before.^{6,14} And since typical $[\text{Ca}^{2+}]$ in vivo is approximately $10^{-6} - 10^{-8}$ M, while that in seawater is about 10 mM,^{15,20} most of the currently developed calcium tracers will reach saturation quickly and therefore are not suitable for calcium measurement in seawater. Therefore, the calcium sensor desired in this project should be characterized with relatively high K_D , i.e. lower affinity to Ca^{2+} comparing to current tracers. As found in the development of tracers for popular divalent ions (Ca^{2+} , Zn^{2+} , etc), most tracers showed capability to bind with other divalent ions besides the target ion.²²⁻²⁴ The prototype of our desired sensor was based on the FluoZin-2 tracer proposed by Gee et al.²⁴ for Zn^{2+} measurement in cells, which is a difluoro- derivative of 6- carboxylfluorescein. The FluoZin-2 sensor showed desired affinity to Ca^{2+} ($K_D \sim 5\text{mM}$), and more importantly it did not show pH dependency within pH unit 6-9 which includes the normal seawater pH. Although the FluoZin-2 molecule was originally designed for Zn^{2+} detection, it was modified from a Ca^{2+} tracer. And furthermore, the Zn ion concentration in seawater is much lower than Ca^{2+} . Hence the structure from Gee's study represents a suitable candidate for our purpose. However, the price of commercially available FluoZin-2 sensor is relatively expensive ($\$397/ 50\mu\text{g}$)³⁹ and thus limits experimental uses. Our purpose in this project is to provide a practical laboratory synthetic method for the calcium sensor, which will be more budget- friendly. The overall synthetic

design is shown as followed (Fig 2), including the synthesis of a calcium ion- binding amine (**3**) and the fluorophore --carboxylfluorescein (**6**). Selection of fluorescein over other groups as the fluorophore mainly due to 1) its large extinction coefficient; 2) high quantum yield; and 3) visible-range excitation and emission wavelength (no UV excitation required).²¹⁻²³

The synthesis of this calcium sensor molecule is the first step of a project collaborated with the School of Marine and Atmospheric Science at Stony Brook University. The final sensor molecule from this step will be further applied to an optical indicator via a polymeric bridge, which is to perform *in situ* measurements.

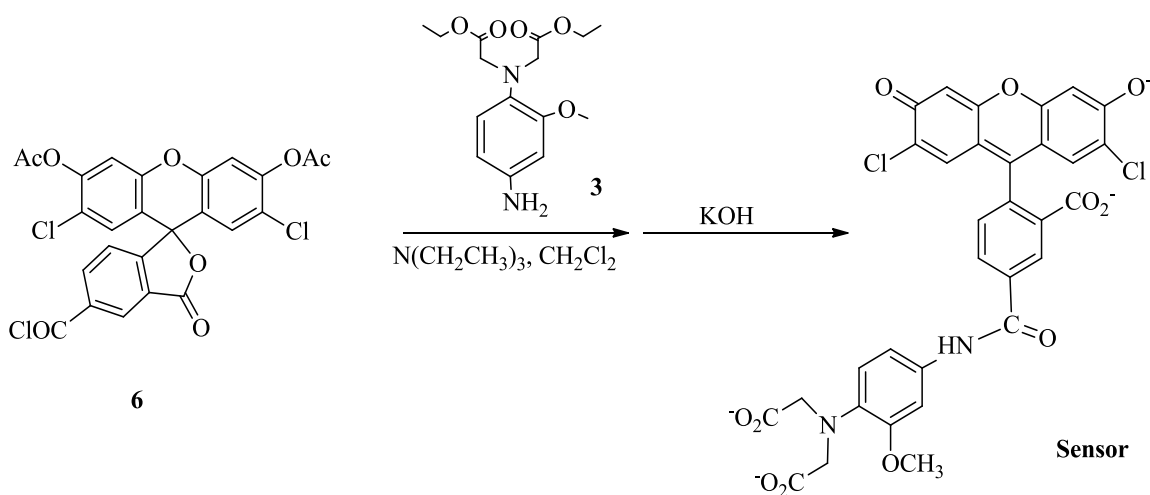
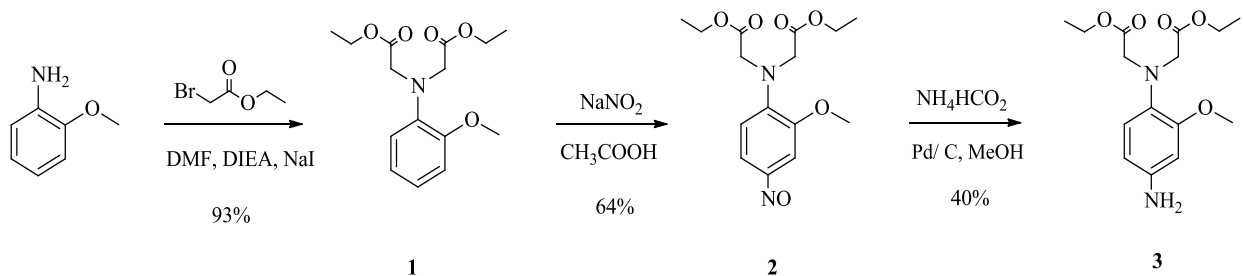


Figure 2. Synthetic design involves the coupling of fluorophore (**6**) with the calcium binding amine (**3**) in dichloromethane. Deprotection of the two acetate groups yields the final product.

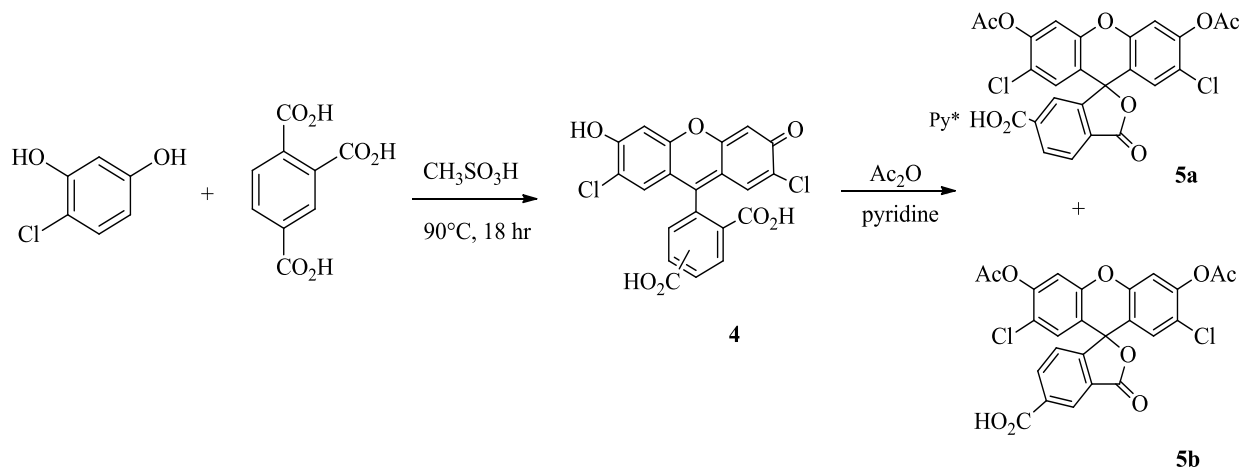
2-2. Overview of Synthetic Route

The complete synthetic route can be mainly divided into three parts: synthesis of calcium binding amine; synthesis of fluorophore; and the coupling of the amine and fluorophore, shown in Scheme 1.

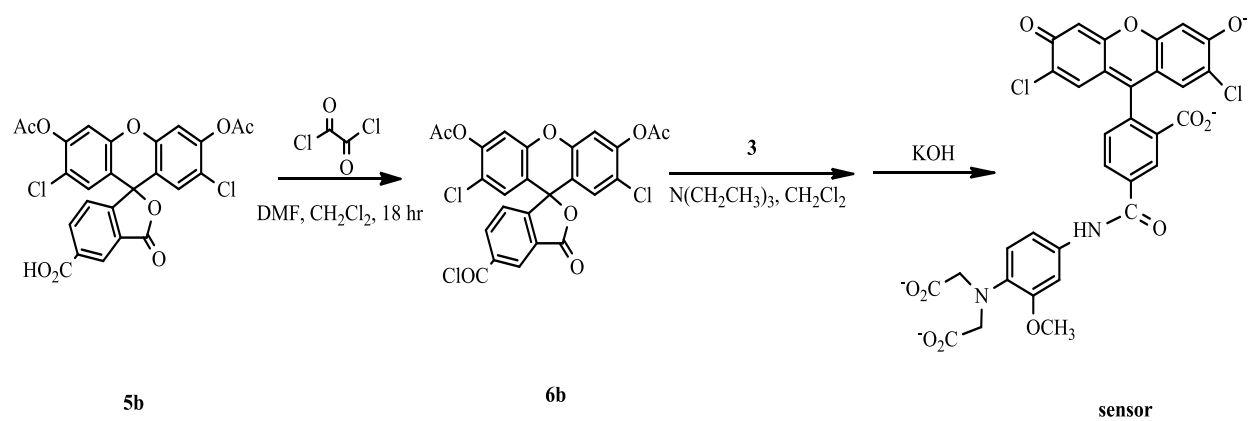
I



II



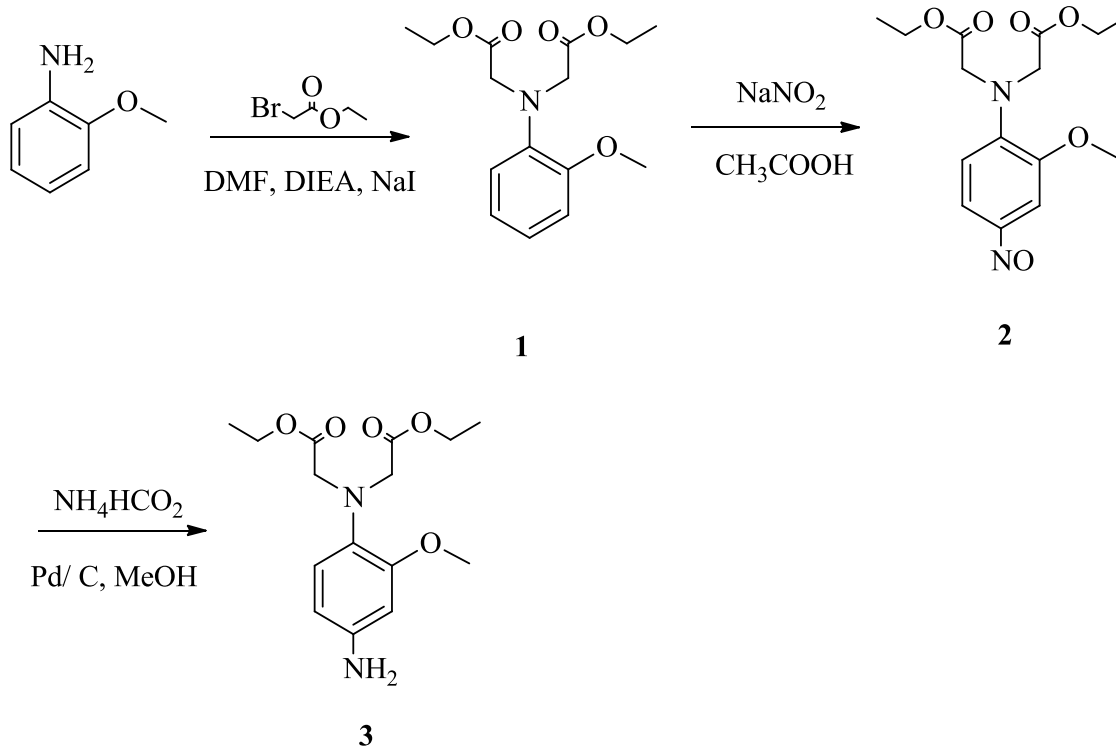
III



Scheme 1. The complete synthetic route includes three main sessions: synthesis of the Ca^{2+} binding amine; synthesis of the fluorophore; and the coupling of the binding amine and the fluorophore

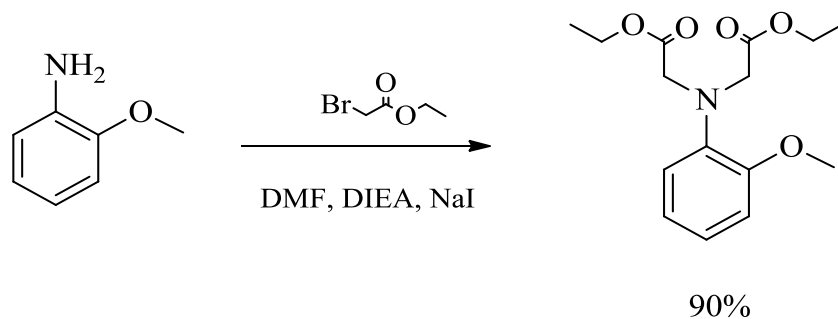
2-3. Results and Discussion

2-3-1. Synthesis of Ca²⁺ Binding Moiety



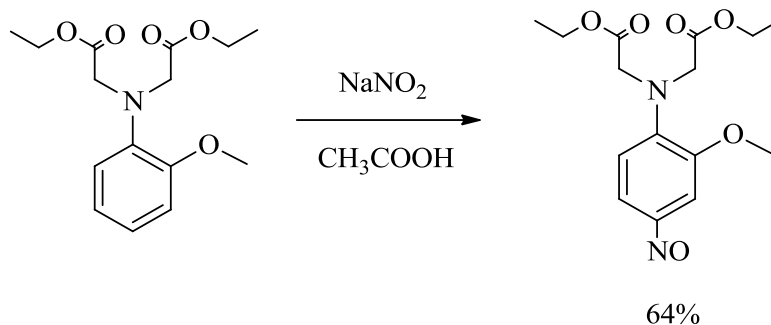
Scheme 2. Detailed scheme of synthesizing Ca²⁺ amine: alkylation of *o*-anisidine; nitrosation; and reduction of the nitroso-compound (**2**).

This part of the synthesis is composed of three steps: production of diethyl 2,2'-((2-methoxyphenyl)azanediyl) diacetate (compound **1**) from alkylation of *o*-anisidine by ethyl bromoacetate²⁵; nitrosation of (**1**) with sodium nitrate for diethyl 2,2'-((2-methoxy-4-nitrosophenyl)azanediyl) diacetate (compound **2**);²⁶ and reduction of (**2**) to yield diethyl 2,2'-((4-amino-2-methoxyphenyl)azanediyl) diacetate (**3**).²⁷



Scheme 3. Step 1: Double alkylation of o-anisidine with ethyl bromoacetate to yield (1).

The first step of alkylation of o-anisidine was successful with about 90% yield calculated. Sodium iodide was added to substitute bromine in ethyl bromoacetate to be a better leaving group, and therefore works as a catalyst. N,N-Diisopropylethylamine was added to serve as a base receiving protons from o-anisidine while it attached to the bromoethyl carbon. A difficulty observed by the previous student in this project was that only 50% of the dialkylation product of o-anisidine was formed, while monoalkylation product accounted for the other 50% (based on ¹H- NMR data).²⁸ Different from this result, integral values of approximately 5.0:3.7 were observed for the two sets of methylene hydrogens adjacent on both sides to the ester group. Such a result suggested that dialkylation was accomplished since each methylene set accounted for four hydrogens attached.



Scheme 4. Step 2: Nitrosation of (1) to yield (2) in acetic acid.

The first attempt to prepare the nitroso-compound (2) was to combine (1) and NaNO_2 with an approximately 1:1 molar ratio in an aqueous solution with glacial acetic acid for 18 hours. The resulted mixture was dissolved in water and extracted with dichloromethane (3X). Organic layers were combined to yield dark brown crude product, which was then analyzed along with starting material (1) in 1:1 ethyl acetate (EA)/ hexane solution on TLC. However, only big spots with an R_f values corresponded to the starting material observed on the product column. Another two trials of TLC were carried out in solutions of 1:9 isopropanol/ hexane and 1:2 isopropanol/ hexane for better separation. However, neither of the two compounds showed sufficient difference in R_f values for analysis. Due to the uncertain results from TLC analysis, the first attempt was suspected not successful and a second try was performed.

Two setups (2- I and 2- II) with different amounts of NaNO_2 added and different reaction time were carried out at the same time for comparison. Detailed information is shown in Table 2. The two crude products were then taken $^1\text{H-NMR}$ spectra after extraction. Both of the crudes appeared to have major peaks for the desired nitroso-compound (2): a doublet at δ 7.8 ppm, a singlet at δ 7.6 ppm, and a doublet at δ 6.8 ppm for the three aromatic hydrogens; a quartet and a single at about δ 4.3 ppm to δ 4.1 ppm for the eight methylene hydrogens from the diacetate; a

triplet at about δ 1.3 ppm for six methyl hydrogens from the diacetate; and a singlet at δ 3.8 ppm for the methyl hydrogens from the methoxyl. Crude 2.2 showed about 50% (based on integrals) of the starting material (**1**) and some other impurities. Crude 2.1 showed dominantly the peaks for the product (**2**). In summary, additional NaNO_2 helped to complete (in high percent yield) the nitrosation, which had a better/ purer result than the reaction of same 1:1 molar ratio of starting material (**1**) and NaNO_2 reacted in extended time. Such an observation may be related to the mechanism of the nitrosation reaction.^{29,30} As shown in Fig.3, the nitrite anion first reacts with two equivalent of protons in an acidic environment and undergoes a hydrolysis to form the nitrosyl cation, which is then later attacked by the electron-rich aromatic ring. Since the acid used in the nitrosation step here is a weak acid (acetic acid) which means the acidic proton does not ionize completely, and the nitrous acid molecule formed from bonding with the first proton is neutral in charge, the second uptake of a proton from the weak acetic acid will not be as efficient. Adding more NaNO_2 therefore, increases the concentration of NO_2^- which would result in more molecular collision and easier to form the nitrosyl cation.

	2- I	2- II
Compound 1	0.51 g (1.7 mmol)	0.50 g (1.7 mmol)
NaNO ₂	0.28 g (4.0 mmol)	0.14 g (2.0 mmol)
CH ₃ CO ₂ H	25 ml	25 ml
H ₂ O	25 ml	25 ml
Time	18 hrs	48 hrs
Temperature	room temp	room temp
R _f Values	starting material (1) 0.56 crude product (2) 0.55	starting material (1) 0.51 crude product (2) 0.56

Table 2. Information of Second Attempt to prepare Diethyl 2,2'-((2-methoxy-4-nitrosophenyl)azanediyl)diacetate (2).

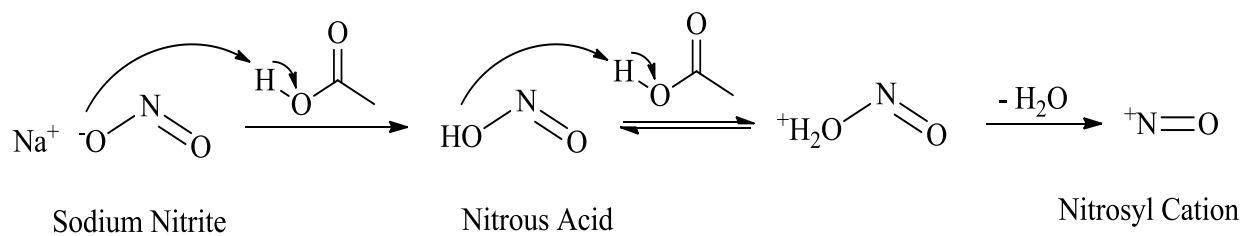
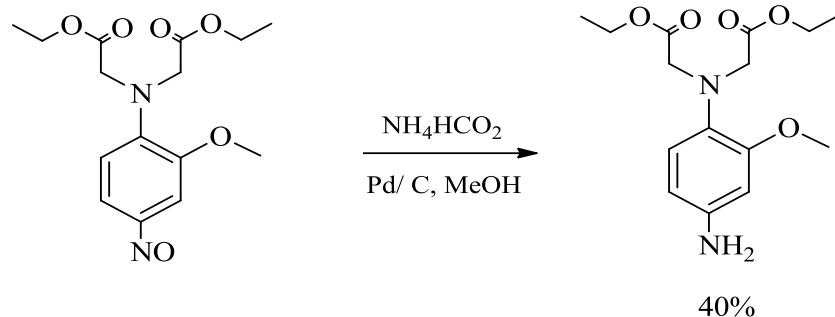


Figure 3. Formation Mechanism of Nitrosyl Cation in Acetic Acid

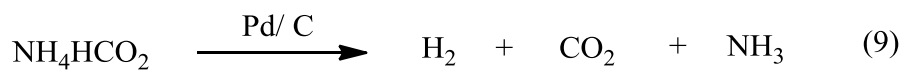


Scheme 5. Step Three: Reduction of (2) to an arylamine (3) ammonium formate on catalysis of Pd/ C.

The final step of Part I converting the nitroso-compound (2) was achieved but with a relatively low yield of no more than 40%. Formates are widely applied hydrogenation/hydrogenolysis in organic experiments since three decades ago, in which they dissociate to yield hydrogen with the presence of Pd/ C and.^{31,33} Ammonium formate catalytic transfer hydrogenation (AF-CTH) gained interest mainly in peptide research due to the ease and rapidness.³¹ Although the detailed mechanism of this system has not yet been thoroughly understood, several relevant studies have been carried out on the topic.³¹⁻³³ The reaction equation shown in Eq. 9 was proposed, and some parameters are thought to affect the process: the amount of hydrogen donor (ammonium formate in this case); the load of Pd on the catalyst; temperature; and types of solvent.^{31,32}

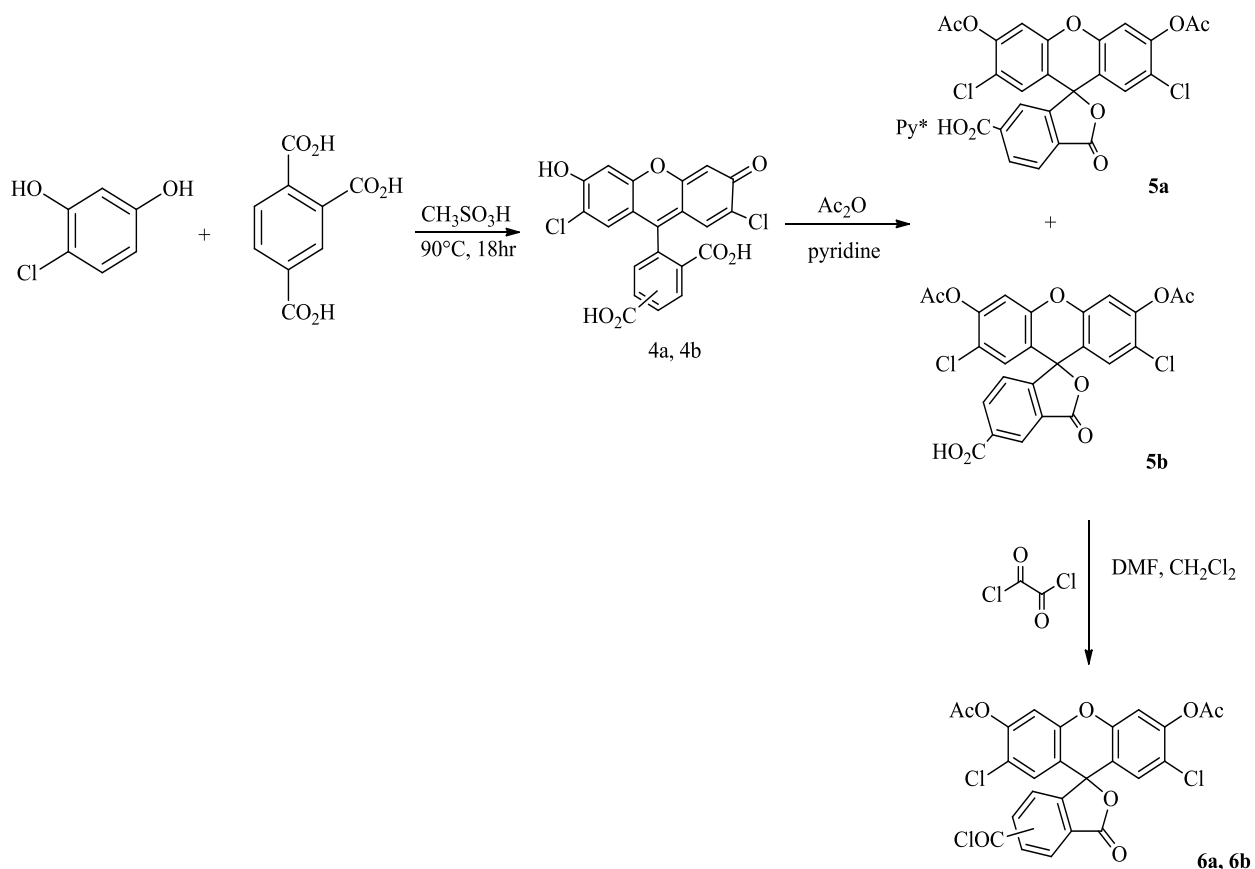
As an original attempt, the starting material (2), AF, and 5% Pd/C were added in a molar ratio of 1: 50 : 1/3 into the solvent of methanol. The reaction was run under ambient temperature for six hours; and 33% yield was obtained. Changes in the aromatic region on ¹H-NMR spectra from (2) to (3) verified the formation of the amine: both the doublet at δ 7.8 ppm and the singlet at δ 7.6 ppm, which represented the two hydrogens ortho to the nitrosyl group, were shifted upfield to around δ 6.2 ppm; while the last hydrogen meta to the nitrosyl was slightly shifted

from δ 6.6 ppm to δ 6.8 ppm. These changes reflected the conversion of $-\text{NO}$ to $-\text{NH}_2$, which is a switch of an electron withdrawing group to a donating group. And the other peaks also appeared to be consistent with the structure. Later 10% Pd / C was used under the same conditions, and a slightly higher yield of 40% was obtained. The low yield of product may also due to loss in the two sequential filtrations (filtered from Pd/ C and from drying agent). Since the Pd/ C powder is quite fine, a large fraction of product might have stucked to the carbon and was difficult to wash off. No further attempts for this reaction were carried out at this point, since the amine (**3**) was formed, and the primary goal was to achieve the synthesis of the sensor. However, a few points can be concluded regarding this reduction reaction. According to the literature in which formate- CTH was applied for another type of reaction (dehalogenolysis),³¹ an amount of 2-fold excess of ammonium formate to the substrate was recommended. The 50-fold amount of ammonium formate to the nitroso- compound should be in a sufficient range for the reduction. And therefore again based on the parameters proposed in the literatures, modifications of Pd/ C amount, temperature and solvent types can be explored in future attempts to improve the yield.

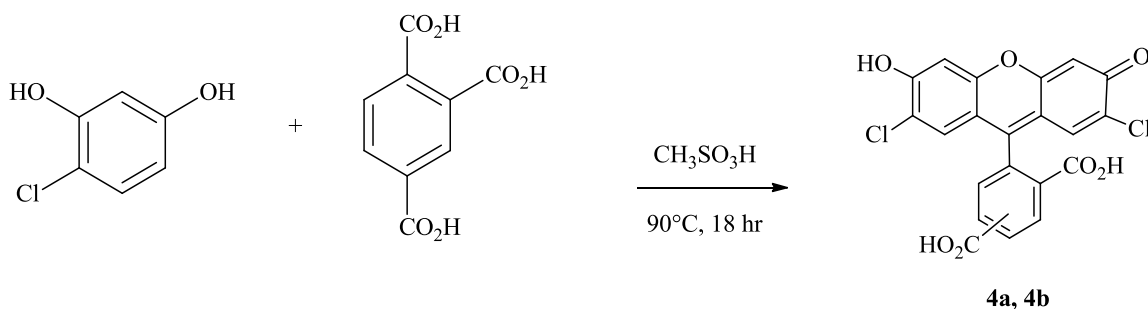


2-3-2. Synthesis of the Fluorophore

The second part of the synthesis also involves three main steps: formation of 2', 7'-dichloro- 5(6) -carboxyfluorescein (**4a**, **4b**), which are two chlorinated isomeric derivatives of the commonly used 5(6) - carboxyfluorescein. Product (**4a**) and (**4b**) were then placed to react with acetic anhydride for protection of the fluorophore, yielding another two isomeric products (**5a**) and (**5b**), with one as a pyridine salt and the other in its pure carboxylic acid form precipitated from water. And lastly the acid product was converted into an acid chloride for coupling with the amine moiety. All the steps in this part were carried out following to the work of Woodrooffe et al.²³

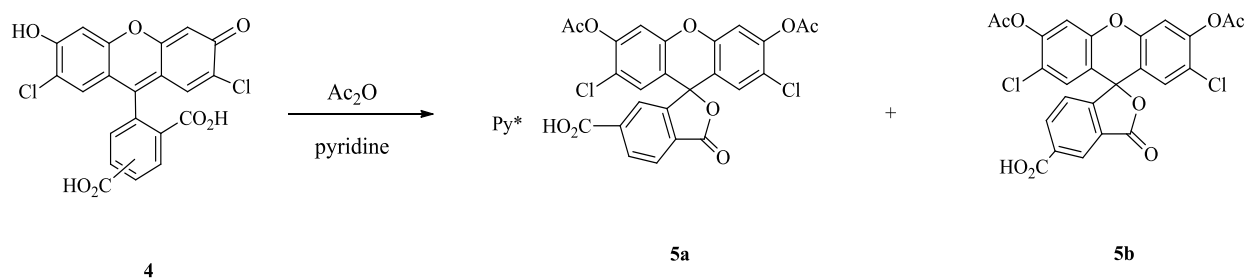


Scheme 6. Detailed scheme of synthesizing the carboxyfluorescein: formation of chlorinated derivatives of 5(6) -carboxyfluorescein (**4a**, **4b**); protection of the carboxyfluorescein; conversion of the acid-form isomer to the acid chloride form.



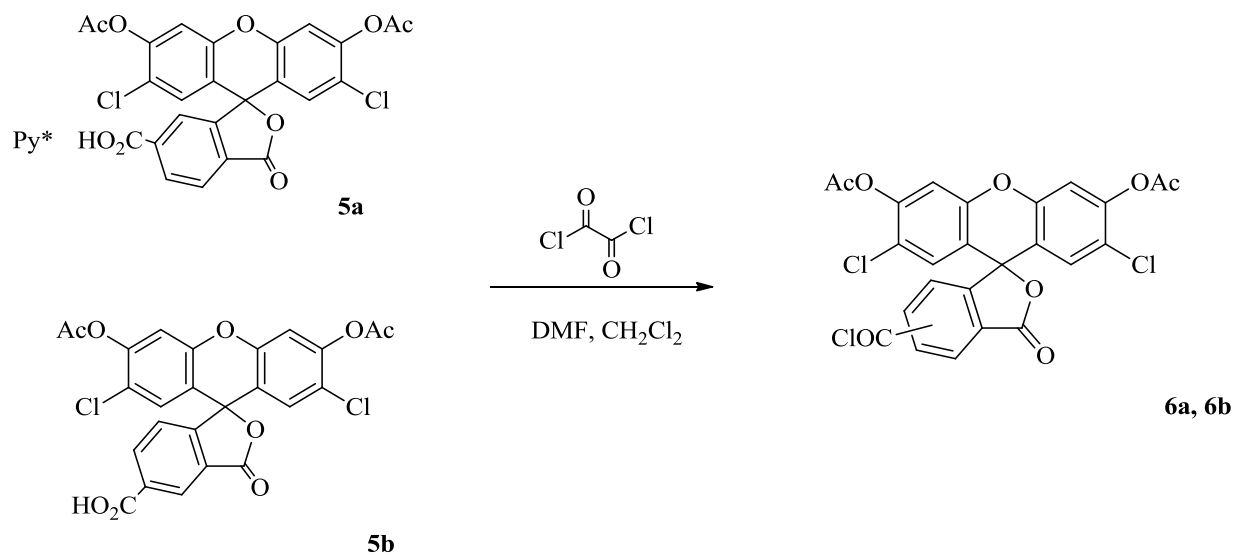
Scheme 7. Step Four: Formation of chlorinated derivatives of 5(6)–carboxyfluorescein (**4a**, **4b**).

4-chloro-resorcinol and 1, 2, 4- benzenetricarboxylic acid were combined in a molar ratio of 2:1 in methanesulfonic acid for a condensation to form the two chlorinated isomeric derivatives of the carboxyfluorescein. Methanesulfonic acid was applied as a non-volatile strong organic acid catalyzing the condensation reaction.³⁵ Due to lack of selectivity on position 1 or 2 in the benzenetricarboxylic acid,²³ either end of the carboxylic acid would react with the electron mass from resorcinol. The final product collected in this step was observed to be an orange solid which was consistent with description in the reference. But the product obtained was not dried through in the later process, resulting in a measured yield slightly more than 100%. The product was carried on to next step without further processing.



Scheme 8. Step Five: Protection of the carboxyfluorescein by acetic anhydride.

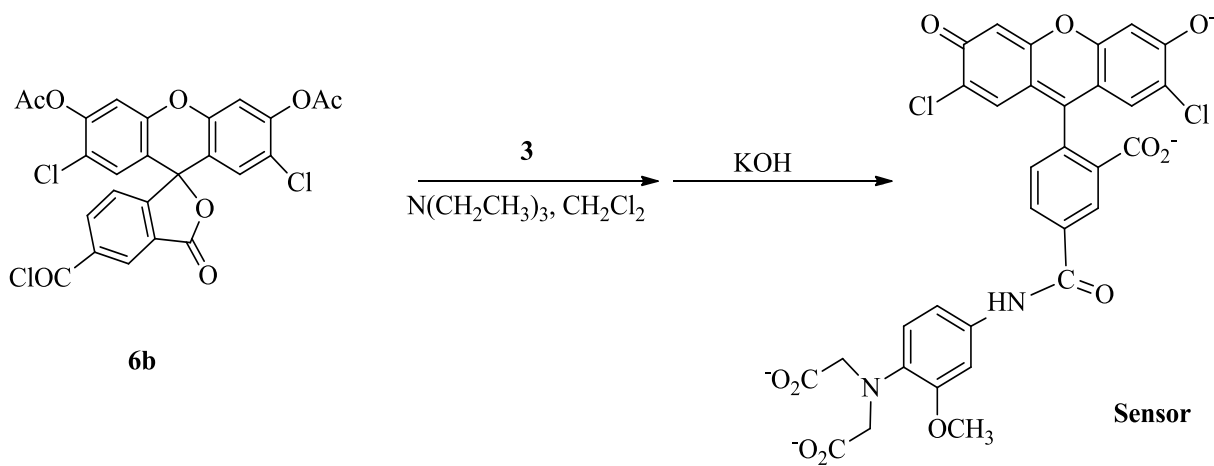
The reactions between the hydroxyl and carbonyl group from the fluorophore were so rapid that change in color (assumably from starting material to product based on description in the reference) was observed, as soon as the acetic anhydride was added. Using pyridine in the reaction may offer two advantage: 1) pyridine acted as a weak base in the system to neutralize the acetic acid formed as a side product, which would interfere later in the conversion to acid chloride; 2) selectively separate the two isomers by different precipitation methods—one as the pyridine salt while the other as carboxylic acid retrieved from organic solvent. The pyridine salt isomer (**5a**) precipitated directly from the reaction mixture, while isomer (**5b**) was precipitated by dissolving the filtrate from (**5a**) in ice water. Success of the reaction was verified by ¹H-NMR comparing to the reference. However, both of the isomers showed large fractions of acetic anhydride and acetic acid: (**5a**) appeared to contain about 27% of Ac₂O and about 18% of AcOH; (**5b**) also appeared to contain about 50% of AcOH. For the purpose of this synthesis (as explained later), isomer (**5b**) was placed under vacuum to further remove the acetic anhydride/ acetic acid. A product up to 80% pure was obtained, while remained acetic acid and other impurities from previous steps still accounted for the other 20%.



Scheme 9. Step Six: Conversion of carboxylfluorescein into an acid chloride form.

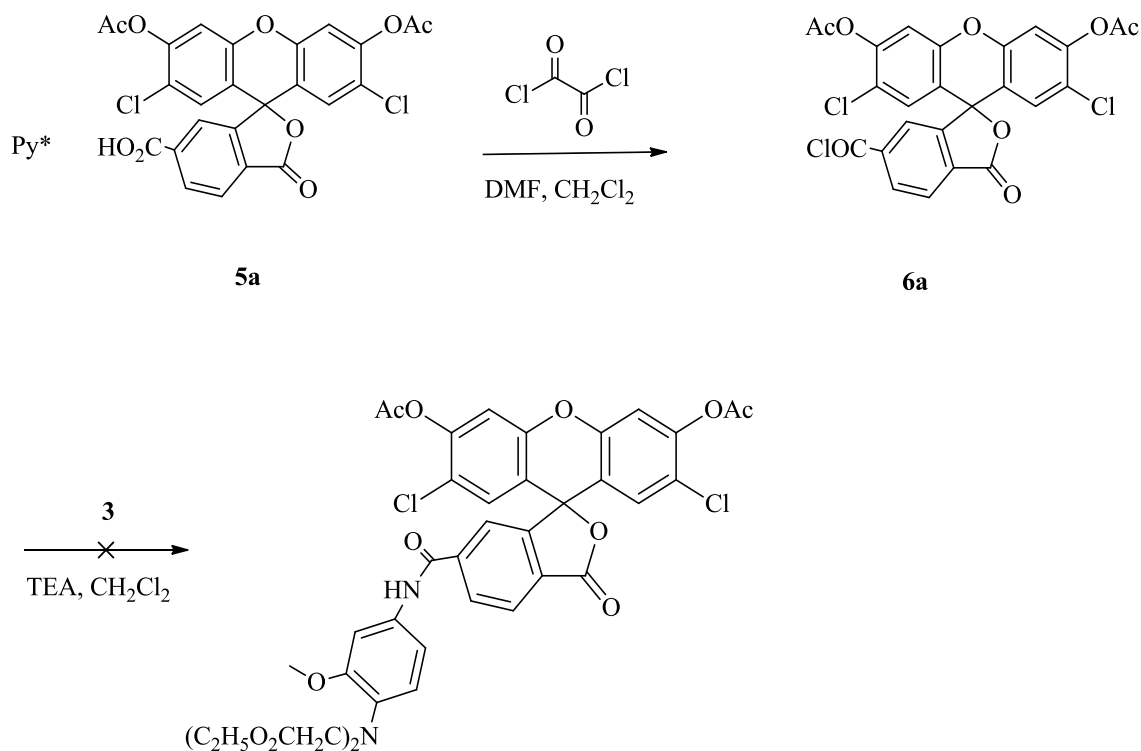
In the conversion of compound (**5a**)/ (**5b**) to their corresponding acid chlorides, the catalyst dimethylformamide (DMF) first reacted with oxalyl chloride to form an intermediate called a Vilsmeier- Haack reagent,³⁶ which was then attacked by the carboxylic acid group. One of the chlorines from oxalyl chloride first reacted with DMF, resulting in the cleavage of oxalyl chloride molecule to form carbon monoxide, carbon dioxide and the other chlorine anion. The unstable Vilsmeier- Haack reagent then reacted with the electron-rich carboxylic group from the fluorophore. An acid chloride product was formed along with the return of a DMF molecule.

2-3-3. Coupling of the Binding amine and the Acid Chloride derivatives of the Fluorophore



Scheme 10. Designed coupling of the amine and fluorophore and deprotection of resulted product.

Using the work of DeRuiter et al.³⁶ as reference, the fluorophore acid chloride (**6**) and the Ca²⁺ binding amine (**3**) was refluxed in anhydrous dichloromethane (DCM) under nitrogen pressure for 12 hours, with triethylamine (TEA) as a base receiving the HCl formed in the reaction. Isomer (**5a**) remained from previous work was mainly used in the reactions from step six and therefore acid chloride (**6a**) was applied in this coupling step, as shown in Scheme 11. Molar ratio of 1: 2: 2.5 for isomer (**5a**): C₂O₂Cl₂ : DMF was applied in the preparation of acid chloride (**6a**); and the ratio for (**6a**): (**3**): TEA was 1: 1: 1.5 in the coupling reaction.



Scheme 11. Coupling from isomer (**5a**).

Several attempts following the procedure mentioned were performed. Since the Ca²⁺ binding amine will change to an amide after coupling, the aromatic hydrogens will become less shielded as the lone pair from nitrogen should be in resonance with the carbonyl and therefore the hydrogen chemical shifts will be more downfield. Such an alteration was the primary key to verify the occurrence of coupling. And the downfield shifts of the amine aromatic hydrogens were indeed observed: the peaks at δ 6.2 ppm from the amine were absent from the position, and together with the peak originally at δ 6.8 ppm mingled in a more left range with other peaks. Although the reaction of the amine seemed promising, whether the shifts of peaks were caused by coupling with the fluorophore was not verified. As a test to figure out whether the two moieties had coupled, a TLC plate spotted with all three substances (**(3)**, **(6a)**, and crude product)

was dipped into a KOH solution for deprotection. Fluorescence was observed in both (**6a**) and the product. And since the product spot appeared to contain a part that was associated to the amine, there was possibility that the two had been reacted. Excessive DMF peaks were also observed suppressing the peaks from product in some trials. Purification of the crude product was carried out in various ratios of EA and hexane. Main peaks of the product remained unseparated by showing broad absorption detected. Also, the purified product appeared to decompose in some instance based on ^1H - NMR. Such results may due to the product's instability on silica column or the overexposure to air.

Attempts with slight modifications to the previous were then carried out. A smaller ratio of DMF and $\text{C}_2\text{O}_2\text{Cl}_2$ were used to get the acid chloride, such that (**5a**): $\text{C}_2\text{O}_2\text{Cl}_2$: DMF was 1: 1 (1.5): 1.5. With these different concentrations, a better ^1H - NMR spectrum was obtained in which the peaks from (**3**) were shown shifted to positions corresponded to the designed amide. However, purification of the product showed separation of the amine and fluorophore. Based on the ^1H - NMR spectrum, shifts of peaks were suspected to be the result of a reaction between the amine and residual acetic acid from previous steps. The proposed structure is as shown in Fig. 4. As a summary up to this point, coupling of the amine to the fluorophore was not achieved due to the competitive interference of acetic acid/ acetic anhydride remained in the fluorophore. Similarly, possible residual oxalyl chloride might have also contributed difficulties to previous coupling attempts (Fig 4).

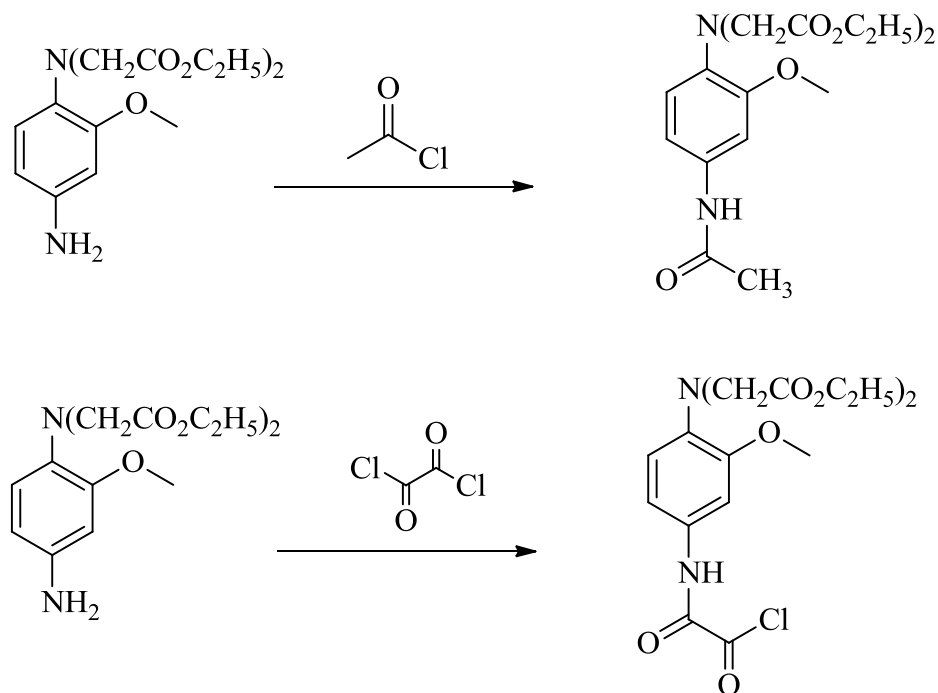
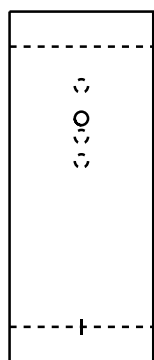


Figure 4. Interference coupling of the residual acetic acid or oxalyl chloride with the Ca²⁺ binding amine (3).

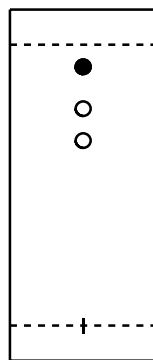
Compound (5a) was placed under vacuum for overnight or equivalent amount of time to remove the excess residual acetic acid. And the acid chloride (6a) was washed with 1, 4- dioxin in order to remove possible remaining oxalyl chloride. Based on ¹H- NMR comparison, about 30% of the acetic acid was removed and the purity of the carboxylic acid appeared to be greater than 90%. A new trial coupling applying these changes in process was carried out. The crude product was purified by column chromatography on silica gel with acetone/ heptane (60%- 80% acetone). The unseparated polar fractions which were suspected containing the desired product were combined. One half of the resulted mixture was spotted on a glass TLC plate for further separation. ¹H- NMR analysis of the obtained bands on the glass plate however, showed mostly only impurity peaks, while the very polar components still remained indistinct. The other half of the mixture was carried on to deprotection. As purification of the polar components in the crude

product appeared hard to accomplish with common solvent combinations, more polar TLC systems were applied.³⁸ The trial systems include: BuOH- AcOH- H₂O, isopropanol- AcOH- H₂O, tert-BuOH- AcOH- H₂O, and CHCl₃- MeOH- H₂O. Detailed ratios were as shown below. BuOH- AcOH- H₂O with ratio 9: 2: 1 showed best separation of each individual spot. Since the purpose was to separate the last polar fractions, CHCl₃- MeOH- H₂O (65: 25: 4 to 65: 25: 10 and 2: 3: 1) were applied in a purification. ¹H- NMR analysis results showed fractionated/ impurity peaks but not that of amine/ fluorophore, which was similar as previous purification.

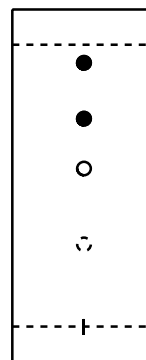
BuOH- AcOH- H₂O



5: 3: 2

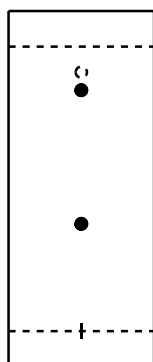


6: 3: 1



9: 2: 1

tert- BuOH -AcOH- H₂O



5: 3: 0.5

CH₃Cl- MeOH- H₂O



65: 25: 4

Figure 5. Polar solvent systems tried for separation of purified fractions with high polarity.

Attempts to verify the coupling reaction were then carried out with some model amines and with the aid of a coupling reagent, dichlorotriphenylphosphorane (DCTPP). *m*-Toluidine was first tried since it has a distinct methyl group attached to the aromatic ring and should give a better signal upon the coupling (rather than being mixed in the aromatic region). The reaction was so rapid that changes of hydrogen peaks on NMR were already observed within 30 minutes. Shifts of the amine aromatic hydrogen peaks were observed as before. However, the methyl

group from m- toluidine has a hydrogen chemical shift of δ 2.29 which is very close to the methyl peak from the fluorophore ($\sim \delta$ 2.38 ppm). Change for these hydrogen appeared to be indistinct from the fluorophore peak. Problem remained as before. According to the work of Azumaya et al.²⁷, dichlorotriphenylphosphorane (DCTPP) was used to synthesize aromatic amide successfully from the corresponding amine and the desired carboxylic acid. It was then tried in the coupling of m- toluidine and fluorophore (**6a**). ¹H- NMR spectra of the purified fractions suggested that the two were not coupled. Another model amine 4- ethylaniline was also applied in the coupling. And a different solvent system ethyl acetate³⁷ was tried as well. None of the result so far was promising. Evidence showed the amine and the fluorophore were not bound.

This predicament led to the reconsideration of the starting materials. Since the aromatic hydrogens from the amine always showed reacted in the reaction, the problem might then focus on the fluorophore. All the attempts before were done with the carboxyfluorescein isomer (**5a**), which was a salt. This property might have restrained the isomer's ability to finish the coupling. Since there was no isomer (**5b**) from previous work found available, a synthesis was carried out to make new isomer (**5b**). Trial coupling of the carboxylic acid isomer (**5b**) with 4- ethylaniline was first carried out. The fluorophore aromatic hydrogen peaks appeared to shift upfield slightly, which matched with the change from an acid chloride to an amide. And the methylene hydrogens in the ethyl group from the amine showed change from δ 2.5 ppm to approximately δ 2.6 ppm; the methyl hydrogens shifted from δ 1.2 ppm to δ 1.3 ppm. Then a coupling reaction using the Ca²⁺ binding amine (**3**) and the fluorophore (**6b**) was carried out following the original procedure in dichloromethane anhydrous with TEA as the base. Similar result to the model coupling with 4- ethylaniline was observed: slight upfield shifts were observed for aromatic hydrogens from the fluorophore; and downfield shifts were observed for that from the amine. The crude product was

then deprotected in KOH solution and neutralized with HCl to maintain the stability of the possible sensor.

Attempts to detect fluorescence intensity of the deprotected product were also performed to first examine the property of the possible product. Starting from the referenced concentration²³ of 1 μM , in the buffer of Trizma (0.1M), decreasing concentration of 0.1 μM and 0.01 μM were measured. All of these samples however, showed saturation fluorescence intensity. A more diluted concentration with 0.01 μM product in the buffer (0.01 M) was tried and a fluorescence reading of 4 (based on the instrument scale) was observed. As a sequential step, a calcium solution was added into the product to see whether there would be an enhancement in fluorescence intensity. A test of the calcium chloride solution alone however, had showed maximum fluorescence. As a result, detection of previous effect was not reliable. Attempts to detect the fluorescence of the possible sensor molecule may need to be carried out on a second instrument for a better insight.

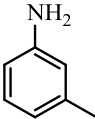
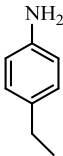
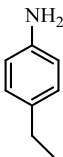
Coupling Attempts			Result
6a	3	(6a)- (3) (molar ratio 1:1) reflux in dichloromethane anhydrous with triethylamine (original procedure)	amine aromatic H peaks changed; but coupling of (6a) and (3) was not confirmed
		smaller ratio of C ₂ O ₂ Cl ₂ and Me ₂ NCOH for preparation of acid chloride; original procedure for coupling	amine aromatic H peaks changed; coupling product from (3) and residual AcOH obtained
6a	 m- toluidine	following original procedure	amine H peaks changed; coupling was not confirmed
		following original procedure with addition of dichloromethylphosphorane	amine H peaks changed; coupling was confirmed not complete
6a	 4- ethylaniline	following recorded procedure	amine H peaks changed; coupling was not confirmed
		following recorded concentration in EA	amine H peaks changed; coupling was confirmed not complete
6b	 4- ethylaniline	following recorded procedure	both amine and fluorophore H peaks observed changes corresponding to the hypothesized product
6b	3	following recorded procedure	both amine and fluorophore H peaks observed changes corresponding to the designed product; coupling suspected achieved

Table 3. Summary of coupling reaction attempts.

2-4. Conclusion and Future Work

In this work a Ca^{2+} sensor for use in marine environment was designed and synthesized. The sensor is designed to give a fluorescent signal upon the binding of calcium ion. The synthetic route was divided into three parts: the synthesis of the Ca^{2+} binding amine (**3**), synthesis of the fluorophore (**6**), and the coupling of the two moieties. Three steps were involved to make the amine (**3**). This synthetic route was proved successful according to the hydrogen NMR data but with an inefficient yield of about 40%. A great deal of effort was put into achieving the coupling between fluorophore isomer (**5a**) and the amine (**3**) and the purification of the resulting product. However, all the results suggested difficulties when using this pyridine salt isomer. Attempt with the other carboxylic isomer on the other hand showed evidence that the desired sensor might have been obtained based on the ^1H - NMR spectrum.

The next step for the process will be to continue detection of fluorescence signal from the coupling product and from its dissolution in a calcium solution; and from that to examine the possible sensor's Ca^{2+} affinity. Improvements for previous synthesis may focus on the synthesis of the Ca^{2+} binding amine (**3**), in which modifications on catalyst amount, temperature and solvent system can be tried.

Chapter Three

Experimental Design and Methods

All the NMR spectra were obtained from a Bruker Fourier 300 NMR spectrometer. The fluorescence detection was performed in an AMINCO • Bowman Series 2 Luminescence Spectrometer, excitation at 505 nm and emission range was between 480 nm and 640 nm.

Diethyl 2,2'-((2-methoxyphenyl)azanediyl) diacetate (**1**)²⁵

o- Anisidine (5.7 mL, 50mmol) and ethyl bromoacetate (16.8 mL 153 mmol) were stirred along with dimethyl formamide (60mL), diisopropyl ethylamine (21 mL,120 mmol), and NaI (7.5g, 50 mmol) at 100°C for 4 hours. The product mixture was dissolved in diethyl ether (100 mL) and extracted with H₂O (2 x 40 mL) and saturated NaCl (aq) solution (20 mL). The organic layer was dried with MgSO₄ and rotary evaporated to give a crude product. The crude product appeared to be a brown oily liquid and was analyzed with TLC (1:1 EA-hexane). R_f 0.46. The mass of the crude product was measured as 13.8g (93% yield). ¹H-NMR (CDCl₃, 300MHz): δ 6.95-6.83 (m, 4H); 4.21-4.18 (q, 4H), J= 7.14Hz; δ4.14 (s, 4H); 3.82 (s, 3H); 1.26 (t, 6H), J= 7.11Hz.

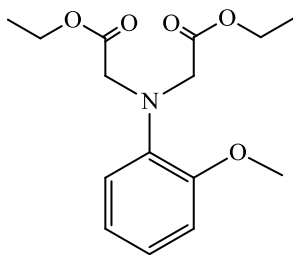


Figure 6. Compound (**1**), diethyl 2,2'-((2-methoxyphenyl)azanediyl) diacetate.

Diethyl 2,2'-((2-methoxy-4-nitrosophenyl)azanediyl)diacetate (**2**)²⁶

Compound 1 (0.5g, 1,7mmol) was dissolved and stirred in a solution of acetic acid (25mL) and H₂O (25mL). NaNO₂ (aq) solution (0.4M, 10 mL) was added to the stirring solution over a time interval of 10 min. The mixture was allowed to react for 18 hours at room temperature. H₂O (40 mL) was added to the yellow crude product and the resulting solution was extracted with CH₂Cl₂ (3 x 50 mL). The organic layer was dried with MgSO₄ and rotary evaporated. The product was purified with silica gel chromatography (50%- 80% CH₂Cl₂ in hexane). Yellow solid product was obtained. The mass was measured as 0.35g (64% yield). TLC analysis was carried out for both crude (1:1 EA- hexane; 10% isopropanol- hexane; 1:1 EA- CH₂Cl₂; CH₂Cl₂) and purified products (CH₂Cl₂). The R_f values for crude product were 0.55, 0.15, 0.05 and 0.47, respectively. ¹H-NMR (CDCl₃, 300MHz): δ 7.84 (dd, 1H), J= 2.28Hz ; δ 7.68 (s, 1H); δ 6.66 (d, 1H), J= 8.91Hz; δ 4.3-4.18 (m, 8H); δ 3.85(s, 3H); δ 1.31 (t, 6H), J= 7.08Hz. m.p. 95 – 97 °C.

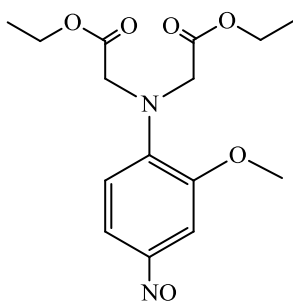


Figure 7. Compound (**2**), diethyl 2,2'-((2-methoxy-4-nitrosophenyl)azanediyl)diacetate.

Diethyl 2,2'-((4-amino-2-methoxyphenyl)azanediyl)diacetate (**3**)²⁷

Compound 2 (0.28g, 0.86 mmol), Pd 5%wt on activated carbon (0.62g) and ammonium formate (2.56 g) were stirred in dry methanol (20 mL). The reaction was carried out at room temperature for 6 hours. The product solution was filtered and the filtrate was dissolved in H₂O (20 mL). The resulting solution was extracted with CH₂Cl₂ (50 mL). The organic layer was dried with MgSO₄ and the solvent was removed by rotary evaporation. Pink solid of 0.107g was obtained. 40% yield. TLC analysis was carried out (60% EA- hexane). The R_f value was 0.24. ¹H-NMR (CDCl₃, 300MHz): δ 6.84 (d, 1H), J= 8.22Hz; δ 6.25- 6.19 (m, 2H); 4.19-4.14 (q, 4H), J= 7.17Hz; δ 4.12 (s, 4H); δ 3.80 (s, 3H); δ 3.68 (s, 3H); δ 1.24 (t, 6H), J= 7.14Hz. m.p. 86 – 88 °C.

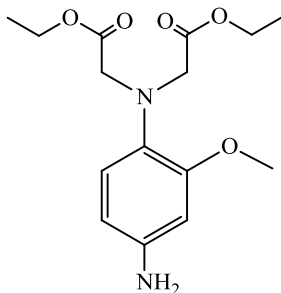


Figure 8. Compound (**3**), diethyl 2,2'-((4-amino-2-methoxyphenyl)azanediyl)diacetate.

2',7'-Dichloro-5(6)- carboxylfluorescein (**4a**, **4b**)²³

4-chlororesorcinol (5.78g, 40mmol) and 1,2,4-benzenetricarboxylic acid (4.20g, 20mmol) were combined in methanesulfonic acid (30mL) and stirred at 90 °C for 18 hours. The mixture was poured into stirred ice water (300mL) and resulting suspension was filtered and washed with water and was dried under vacuum at 90 °C overnight. Orange solid of 18g was obtained, which is more than the theoretical yield, indicating the presence of impurities. The crude product was used in the next step without further purification or characterization.

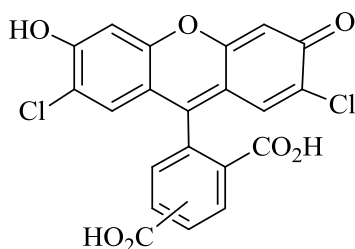


Figure 9. Compound (**4a**, **4b**), 2',7'-Dichloro-5(6)- carboxylfluorescein.

3',6'-diacetyl-2',7'-dichloro-6-carboxyfluorescein pyridine salt (**5a**)²³

Compound 4 (17.84g) was dissolved in acetic anhydride (30mL) and pyridine (2mL) and heated to reflux for 30 minutes. The reaction was cooled to room temperature for 24 hours and filtered. A very small amount of white flake-like solid was collected. Filtration for a second time was performed after another 2 hours. Again only a little portion of precipitate collected. Total weight was less than 0.3g. ¹H-NMR (CDCl₃, 300MHz): δ 8.70 (s, 2H); δ 8.44 (d, 1H), J= 7.95Hz; δ 8.16 (d, 1H), J= 7.95Hz; δ 7.92 (s, 1H); δ 7.85 (m, 1H); δ 7.46- 7.44 (m, 2H); δ 7.18 (s, 2H); 6.88 (s, 2H); 2.38 (s, 6H).²³ m.p. > 230 °C.

3',6'-diacetyl-2',7'-dichloro-5-carboxyfluorescein (**5b**)²³

To the filtrate liquid 60mL of water was added slowly with stirring. Ethyl acetate (30 mL) was added to dissolve the mass formed and another 90ml (30 mL x 3) of ethyl acetate was used for extraction. The organic layer was washed with 10% hydrochloric acid (30 mL) and brine (20 mL). The solution was dried over magnesium sulfate and rotary evaporated. Yellow solid with a mass of 5.75g was obtained. 108% yield. ¹H-NMR (CDCl₃, 300MHz): δ 8.81 (s, 1H); δ 8.48 (d, 1H), J= 1.17Hz; δ 7.35(d, 1H), J= 8.04Hz; δ7.19 (s, 2H); δ6.88 (s, 2H); δ 2.39 (s, 6H); 2.14 (s, 3H).²³ m.p. 148 – 150 °C.

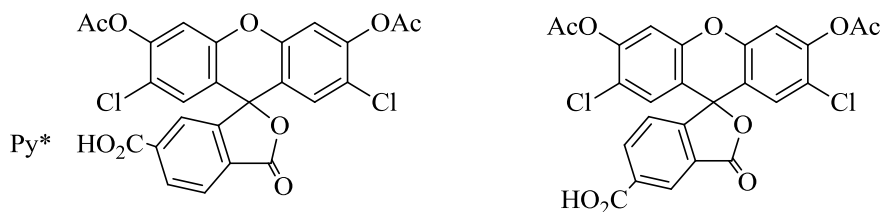


Figure 10. Compound (**5a**, **5b**), 3',6'-diacetyl-2',7'-dichloro-6-carboxyfluorescein pyridine salt and 3',6'-diacetyl-2',7'-dichloro-5-carboxyfluorescein

2',7'-dichloro-6-(chlorocarbonyl)-3-oxo-3H-spiro[isobenzofuran-1,9'-xanthene]-3',6'-diyl diacetate (**6a**)²³

Compound **5a** (1.77g, 3 mmol) was dissolved in dry CH₂Cl₂ (30 mL) and stirred at ice temperature. N,N dimethylformamide (0.347 mL, 4.5 mmol) and 98% oxalyl chloride (0.386 mL, 4.5 mmol) were added to the mixture. Reaction was stirred for 18 hours under nitrogen. Product was rotary evaporated and appeared as yellow solid. ¹H-NMR (CDCl₃, 300MHz): δ8.86 (m, 2H); δ8.48- 8.40 (m, 2H); δ8.17 (d, 1H), J= 7.77Hz; δ 8.06 (s, 1H); δ 8.01- 7.97 (m, 2H); δ 7.19 (s, 2H) δ6.87 (s, 2H); δ 2.38 (s, 6H)

2',7'-dichloro-5-(chlorocarbonyl)-3-oxo-3H-spiro[isobenzofuran-1,9'-xanthene]-3',6'-diyl diacetate (**6b**)²³

Compound **5b** (0.40g, 0.57 mmol) was dissolved in dry CH₂Cl₂ (8 mL) and stirred at ice temperature. N,N dimethylformamide (0.133 mL, 1.72 mmol) and 98% oxalyl chloride (0.1mL, 1.16 mmol) were added to the mixture. Reaction was stirred for 18 hours under nitrogen pressure. Product was rotary evaporated and appeared as yellow solid. ¹H-NMR (CDCl₃, 300MHz): δ8.84 (s, 1H); δ 8.45 (d, 1H), J= 8.07 Hz; δ 7.38 (d, 1H), J= 8.16Hz; δ 7.20 (s, 2H); δ 6.68 (s, 2H); δ 2.39 (s, 8H)

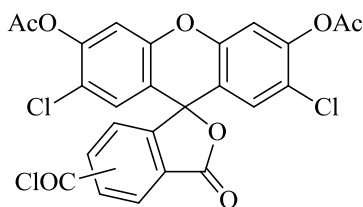


Figure 11. Compound (**6a**, **6b**), 2',7'-dichloro-5(6)-(chlorocarbonyl)-3-oxo-3H-spiro[isobenzofuran-1,9'-xanthene]-3',6'-diyl diacetate.

Diethyl 2,2'-((4-(3',6'-diacetoxy-2',7'-dichloro-3-oxo-3H-spiro[isobenzofuran-1,9'-xanthen]-6-ylcarboxamido)-2-methoxyphenyl)azanediyl)diacetate (**sensor**)²⁴

Acid- chloride form fluorophore (**6b**) (0.57 mmol) was vacuum pumped and dissolved in dry CH₂Cl₂ (8 mL) under nitrogen pressure. The calcium binding amine (**3**) (0.156g, 0.5 mmol) was vacuum pumped and placed under nitrogen pressure in a separate round bottom flask. Triethylamine (0.114 mL, 1.43 mmol) was added along with the fluorophore solution into the amine. The mixture was refluxed at 45°C for 12 hours. Dark red product mixture was obtained. ¹H-NMR (CDCl₃, 300MHz): δ 8.55 (s, 1H); δ 8.34 (d, 1H), J= 8.01 Hz; δ 7.37 (d, 1H), J= 8.34Hz; δ 7.19 (s, 2H); δ 6.90- 6.86 (m, 4H); δ 4.19-4.17 (m, 8H); δ 3.85 (s, 3H); δ 2.39 (s, 6H).

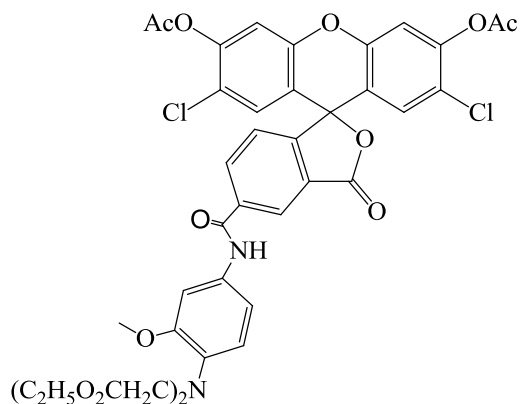


Figure 12. Designed protected sensor structure, diethyl 2,2'-((4-(3',6'-diacetoxy-2',7'-dichloro-3-oxo-3H-spiro[isobenzofuran-1,9'-xanthen]-6-ylcarboxamido)-2-methoxyphenyl)azanediyl)diacetate.

Deprotection Step

Amine- fluorophore coupling product (0.5 mmol) was dissolved in ethanol (1.5 mL) and KOH solution (4M, 0.3 mL). The mixture was covered with aluminum foil and stirred at room temperature for 4 hours. The mixture was then dry under rotary evaporation and dissolved in H₂O (1.2 mL). Hydrochloric acid (2M, 0.1 mL) was added to acidify the pH to 5.6.

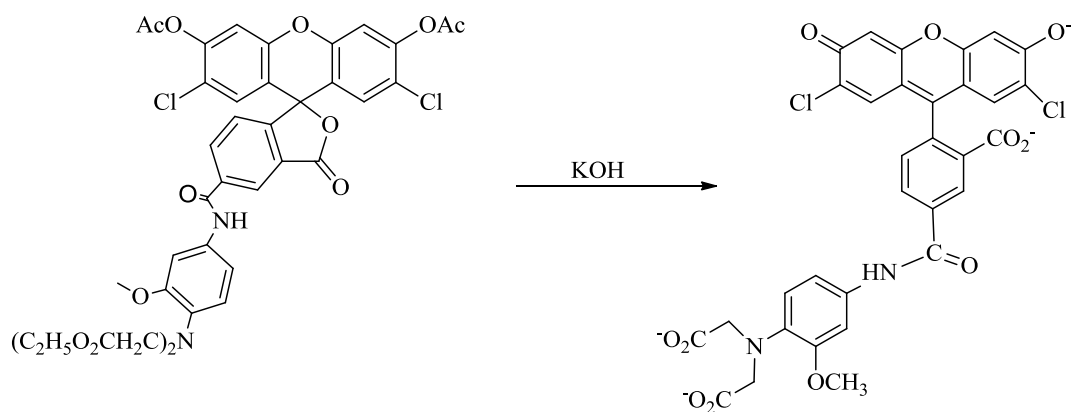


Figure 13. Designed deprotection of crude sensor.

References

1. Dickson A. G. The carbon dioxide system in seawater: equilibrium chemistry and measurements. In *Guide to best practices for ocean acidification research and data reporting*; Riebesell U., Fabry V. J., Hansson L. & Gattuso J.-P. (Eds.), Luxembourg: Publications Office of the European Union. 2010. pp 17- 40.
2. Farley R.H. Chemistry and the Aquarium: Calcium. *Advanced Aquarists* [Online] 2002, 1(3) <http://www.advancedaquarist.com/2002/3/chemistry> (accessed Jul. 6, 2013)
3. Feely, R.A., Sabine, C.L., Lee, K., Berelson, W., Kleypas, J., Fabry, V.J., and Millero, F.J. Impact of anthropogenic CO₂ on the CaCO₃ system in the oceans. *Science*, 2004. 305(5682): p. 362-366.
4. Kump, L.R., T.J. Bralower, and A. Ridgwell. Ocean acidification in deep time. *Oceanography*, 2009. 22. p. 94 – 107.
5. Fabry, V.J., Seibel, B.A., Feely, R.A., and Orr, J.C. Impacts of ocean acidification on marine fauna and ecosystem processes. *ICES Journal of Marine Science: Journal du Conseil*, 2008. 65(3): p. 414-432.
6. Doney, S.C., Fabry, V.J., Feely, R.A., and Kleypas, J.A. Ocean acidification: the other CO₂ problem. *Marine Science*, 2009. 1.
7. Sabine, C.L., Feely, R.A., Gruber, N., Key, R.M., Lee, K., Bullister, J.B., Wanninkhof, R., Wong, C.S., Wallace, D.W.R., Tilbrook, B., Millero, F.J., Peng, T-H., Kozyr, A., Ono, T., and Rios, A. The oceanic sink for anthropogenic CO₂. *Science*, 2004. 305(5682): p. 367-371.
8. Millero, F.J. The marine inorganic carbon cycle. *Chemical reviews*, 2007. 107(2): p. 308-341.
9. Millero, F.J. Thermodynamics of the carbon dioxide system in the oceans. *Geochimica et Cosmochimica Acta*, 1995. 59(4): p. 661-677.
10. Green, M.A., Jones, M.E., Boudreau, C.L., and Moore, R.L., Westman, B.A. Dissolution mortality of juvenile bivalves in coastal marine deposits. *Limnology and Oceanography*, 2004. 49(3): p. 727-734.
11. Orr, J.C., Fabry, V.J., Aumont, O., Bopp, L., Doney, S.C., Feely, R.A., Gnanadesikan, A., Gruber, N., Ishida, A., Joos, F., Key, R.M., Lindsay, K., Reimer, E.M., Matear, R., Monfray, P., Mouchet, A., Najjar, R.G., Plattner, G.K., Rodgers, K.B., Sabine, C.L., Sarmiento, J.L., Schlitzer, R., Slater, R.D., Totterdell, I.J., Weirig, M-F., Yamanaka, Y., and Yool, A. Anthropogenic ocean acidification over the twenty-first century and its impact on calcifying organisms. *Nature*, 2005. 437(7059): p. 681-686.
12. Kuffner, I.B., Andersson, A.J., Jokiel, P., Rodgers, K., and Mackenzie, M.T. Decreased abundance of crustose coralline algae due to ocean acidification. *Nature Geoscience*, 2007. 1(2): p. 114-117.

13. Marshall, A.T. and P.L. Clode, Effect of increased calcium concentration in sea water on calcification and photosynthesis in the scleractinian coral *Galaxea fascicularis*. *Journal of Experimental Biology*, 2002. 205(14): p. 2107-2113.
14. Protopopescu, N. O. Development of a Ca^{2+} Planar Sensor And Application to Early Diagenetic Processes. PhD Proposal. State University of New York at Stony Brook, NY.
15. Tsien, R.Y., New calcium indicators and buffers with high selectivity against magnesium and protons: design, synthesis, and properties of prototype structures. *Biochemistry*, 1980. 19(11): p. 2396-2404.
16. Decuyper J-P, Kindt D, Luyten T, Welkenhuyzen K, Missiaen L., Smedt, H.D., Bultynck, G., and Parys, J.B. (2013) mTOR-Controlled Autophagy Requires Intracellular Ca^{2+} Signaling. *PLoS ONE* 8(4): e61020. doi:10.1371/journal.pone.0061020
17. Grynkiewicz, G., M. Poenie, and R.Y. Tsien. A new generation of Ca^{2+} indicators with greatly improved fluorescence properties. *Journal of Biological Chemistry*, 1985. 260(6): p. 3440-3450.
18. Zou, J., Hofer, A. M., Lurtz, M. M., Gadda, G., Ellis, A. L., Chen, N., Huang, Y., Holder, A., Ye, Y., Louis, C. F., Welshhans, K., Rehder, V., and Yang, J. J. 2007. Developing Sensors for Real-Time Measurement of High Ca^{2+} Concentrations. *Biochemistry*. 46: 12275-12288.
19. Gerasimenko, O. and A. Tepikin, How to measure Ca^{2+} in cellular organelles? *Cell Calcium*, 2005. 38(3): p. 201-211.
20. Silva, J. and R. Williams. *The biological chemistry of the elements: the inorganic chemistry of life*; Oxford University Press: Great Britain, 2001.
21. Sun, W.-C., Gee, K.R., Klaubert, D.H., and Haugland, R.P. Synthesis of fluorinated fluoresceins. *The Journal of Organic Chemistry*, 1997. 62(19): p. 6469-6475.
22. Walkup, G.K., Burdette, S.C., Lippard, S.J., and Tsien, R.Y. A new cell-permeable fluorescent probe for Zn^{2+} . *Journal of the American Chemical Society*, 2000. 122(23): p. 5644-5645.
23. Woodrooffe, C.C., Masalha, R., Barnes, K.R., Frederickson, C.J., and Lippard, S.J. Membrane- Permeable and –Impermeable Sensors of the Zinpyr Family and Their Application to Imaging of Hippocampal Zinc In Vivo. *Chemistry & Biology*, 2004. 11(12): p. 1659- 1666
24. Gee, K.R., Zhou, Z.L., Ton-That, D., Sensi, S.L., and Weiss, J.H. Measuring zinc in living cells: A new generation of sensitive and selective fluorescent probes. *Cell calcium*, 2002. 31(5): p. 245-251.
25. Que, E.L. and C.J. Chang. A smart magnetic resonance contrast agent for selective copper sensing. *Journal of the American Chemical Society*, 2006. 128(50): p. 15942-15943.
26. Gunnlaugsson, T., Nima Gunaratne, H.Q., Nieuwenhuyzen, M., and Leonard, J.P. Synthesis of functionalised macrocyclic compounds as Na^{+} and K^{+} receptors: a mild and high yielding

nitration in water of mono and bis 2-methoxyaniline functionalised crown ethers. *Journal of the Chemical Society, Perkin Transactions 1*, 2002(17): p. 1954-1962.

27. Azumaya, I., Okamoto, T., Imabeppu, F., and Takayanagi, H. Simple and convenient synthesis of tertiary benzanilides using dichlorotriphenylphosphorane. *Tetrahedron*, 2003. 59(13): p. 2325-2331.

28. Wu, L. Development of a Fluorescent Calcium (Ca^{2+}) Sensor to Investigate Marine Sedimentary Conditions. Senior Research Report. State University of New York at Stony Brook, NY. May, 2009

29. Hunt, I. Dept. of Chemistry, University of Calgary. Chap 22. Amines, Nitrosation of Amines. <http://www.chem.ucalgary.ca/courses/351/Carey5th/Ch22/ch22-3-6.html>. (accessed Jul 6, 2013)

30. Solomons, T.W., Fryhle, C.B. *Organic Chemistry*, 9th ed.; Wiley, United States. 2008. pp 919- 26

31. Anwer, M.K., Sherman, D.B., Roney, J.G., and Spatola, A.F. Applications of ammonium formate catalytic transfer hydrogenation. 6. Analysis of catalyst, donor quantity, and solvent effects upon the efficacy of dechlorination. *The Journal of Organic Chemistry*, 1989. 54(6): p. 1284-1289.

32. Dobrovolna, Z. and L. Červený. Ammonium formate decomposition using palladium catalyst. *Research on Chemical Intermediates*, 2000. 26(5): p. 489-497.

33. Rajagopal, S. and A. Spatola. Mechanism of palladium-catalyzed transfer hydrogenolysis of aryl chlorides by formate salts. *The Journal of Organic Chemistry*, 1995. 60(5): p. 1347-1355.

34. Pak, J. Synthesis of a Fluorescent Calcium Sensor for the Environmental Research of the Ocean and the Ecosystem. Senior Research Report. State University of New York at Stony Brook, NY. May, 2011

35. Guthrie, J.P. Hydrolysis of esters of oxy acids: p K a values for strong acids; Brønsted relationship for attack of water at methyl; free energies of hydrolysis of esters of oxy acids; and a linear relationship between free energy of hydrolysis and p K a holding over a range of 20 p K units. *Canadian Journal of Chemistry*, 1978. 56(17): p. 2342-2354.

36. DeRuiter, J., Swearingen, B.E., Wandrekar, V., and Mayfield, C.A. Synthesis and in vitro aldose reductase inhibitory activity of compounds containing an N-acylglycine moiety. *Journal of medicinal chemistry*, 1989. 32(5): p. 1033-1038.

37. Ueda, S. and H. Nagasawa. Copper-catalyzed synthesis of benzoxazoles via a regioselective C– H functionalization/C– O bond formation under an air atmosphere. *The Journal of organic chemistry*, 2009. 74(11): p. 4272-4277.

38. ResearchGate. What is the best way to isolate compounds from MeOH extracts of leaves? http://www.researchgate.net/post/What_is_the_best_way_to_isolate_compounds_from_MeOH_extracts_of_leaves. (accessed Jul 6, 2013)

39. FluoZin™-2, AM, cell permeant, life technologies™.
<http://products.invitrogen.com/ivgn/product/F24189> (accessed Jul 6, 2013)

Appendices

¹H- NMR Spectra of Compounds

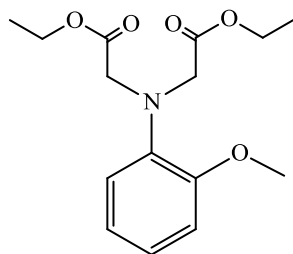
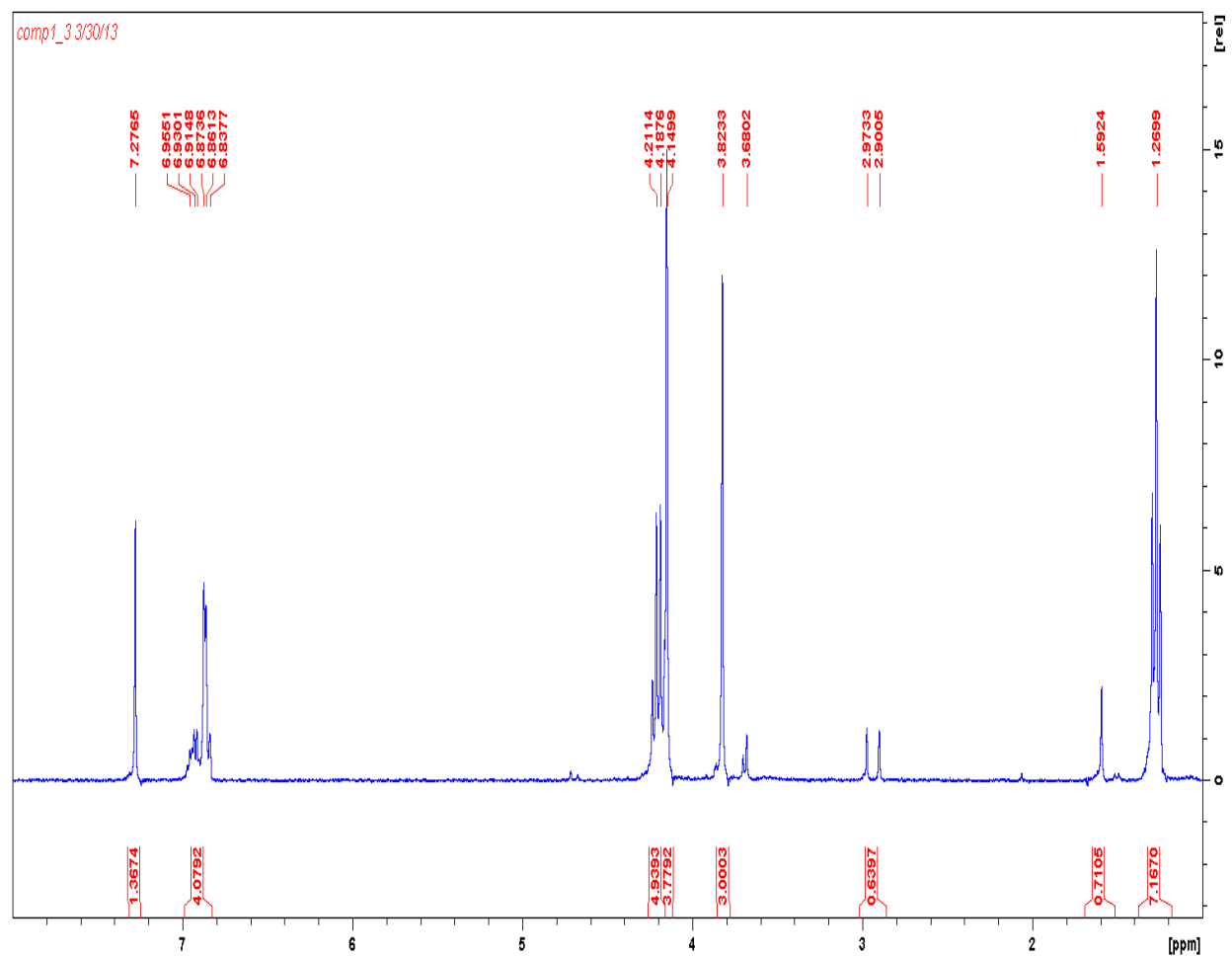


Figure 14. ¹H- NMR spectrum of compound (1) in chloroform- d.

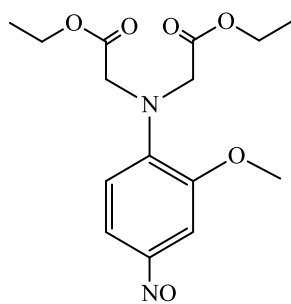
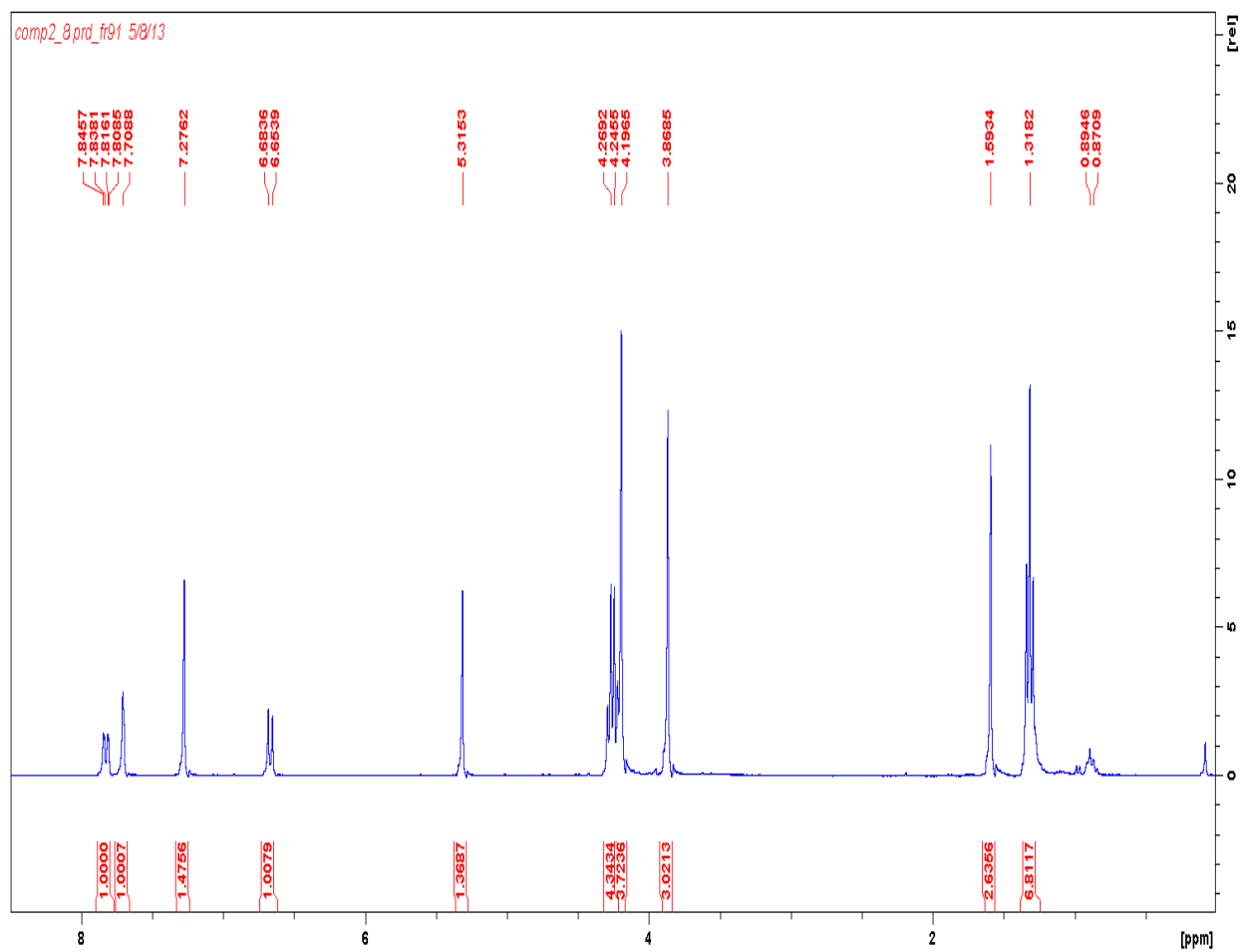


Figure 15. ¹H- NMR spectrum of compound (2) in chloroform- d.

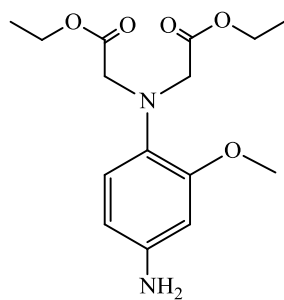
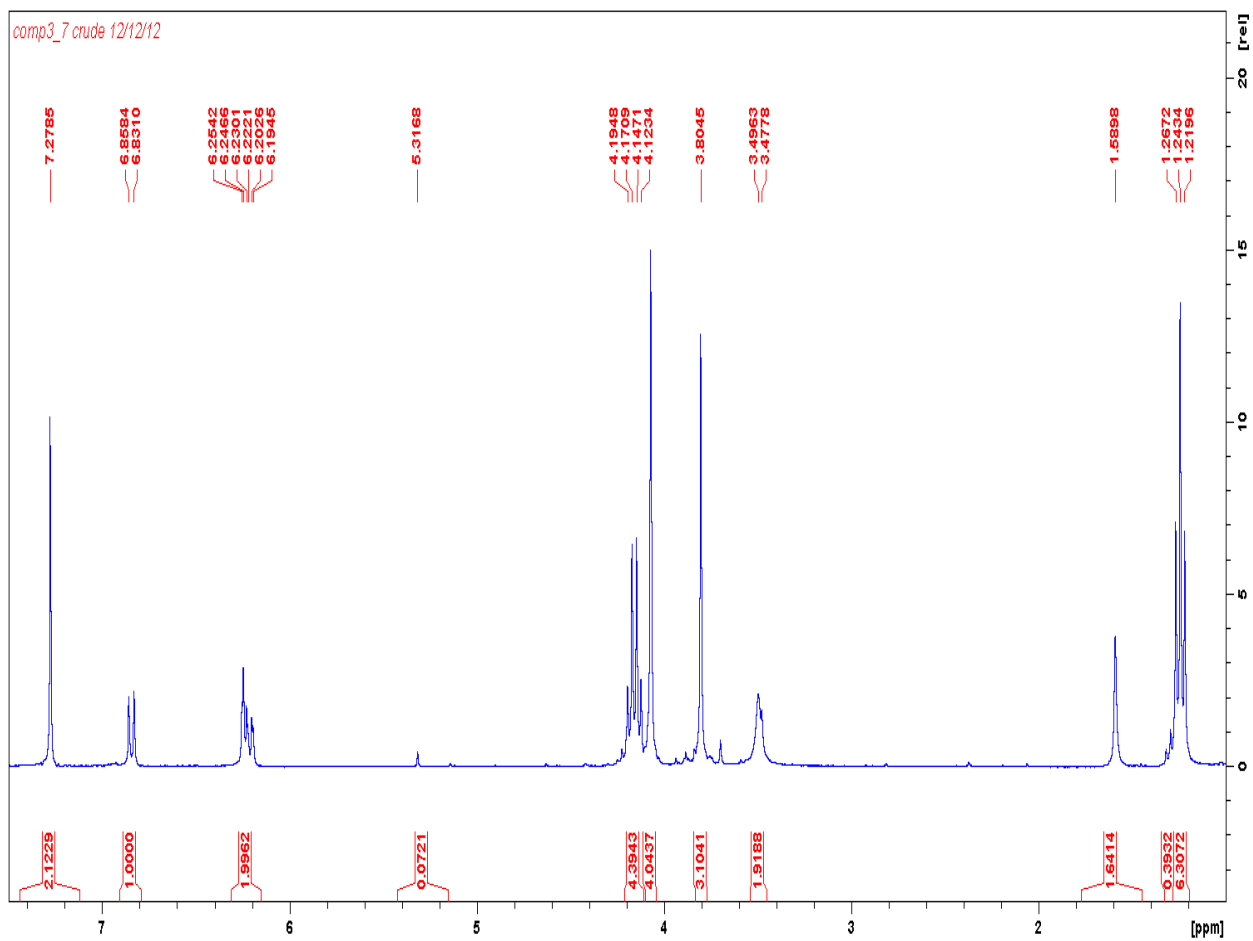


Figure 16. ^1H -NMR spectrum of compound (**3**) in chloroform- d .

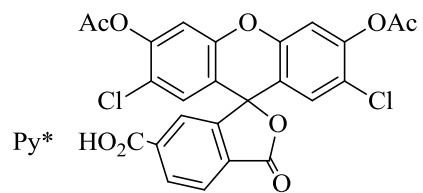
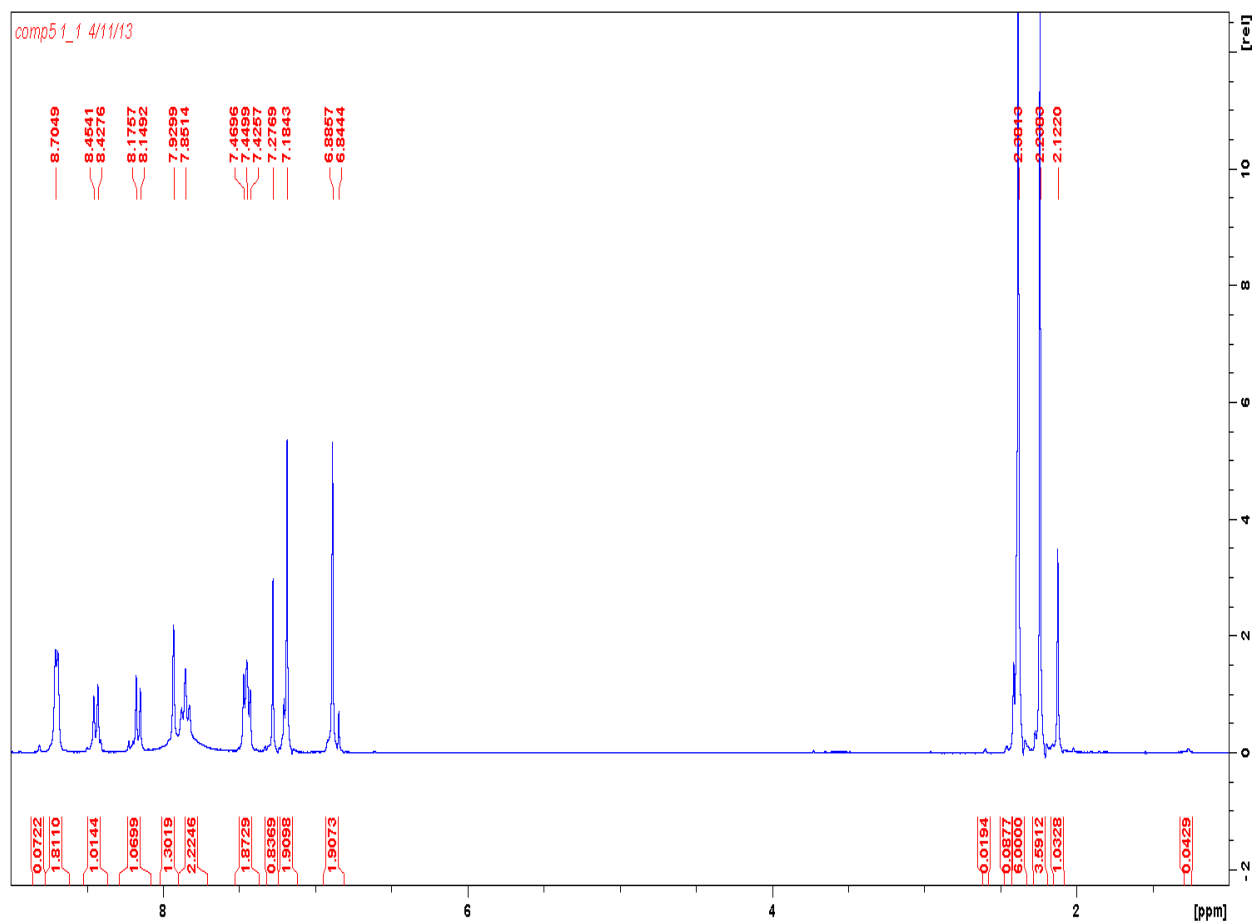


Figure 17. ^1H - NMR spectrum of compound (**5a**) in chloroform- d .

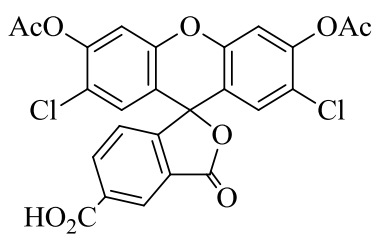
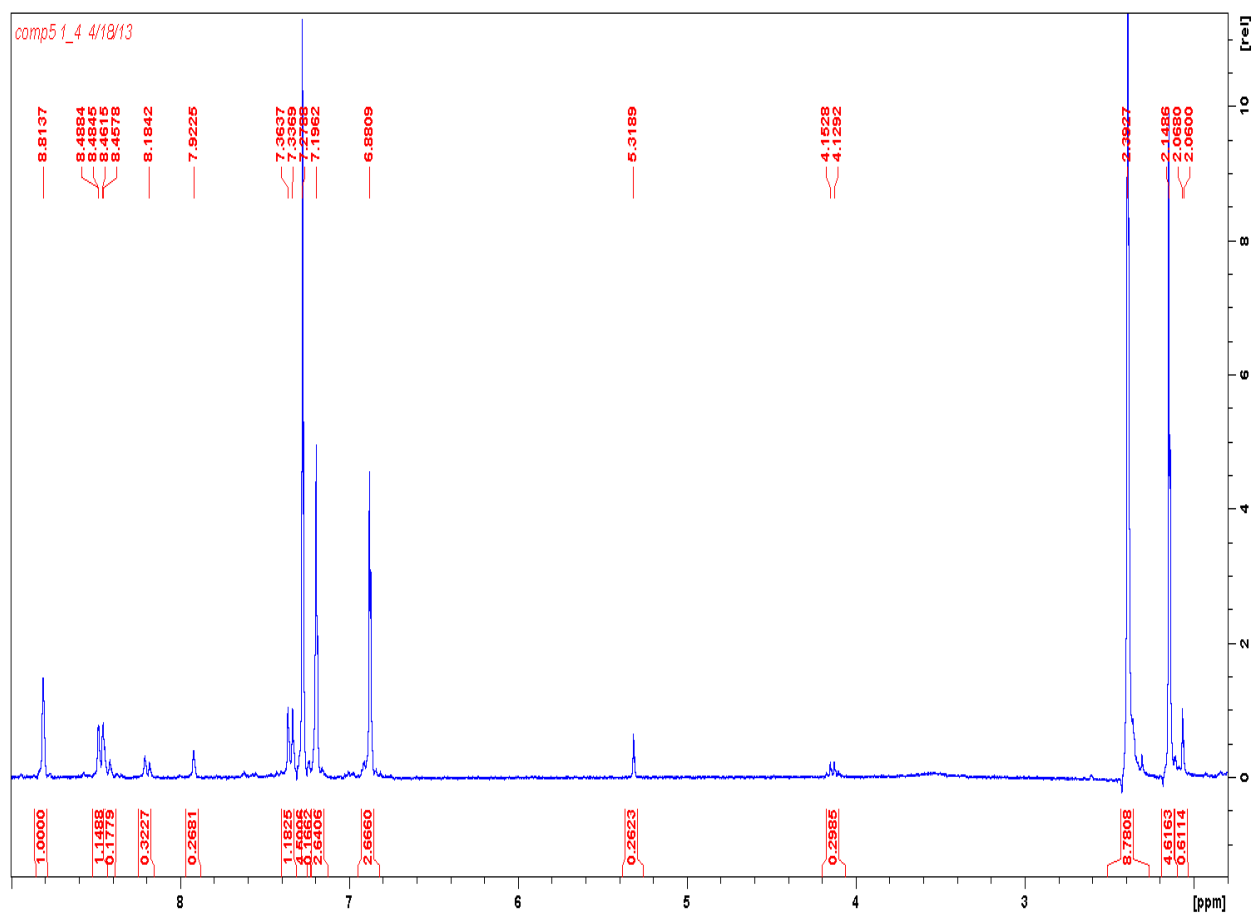


Figure 18. ^1H -NMR spectrum of compound (5b) in chloroform- d.

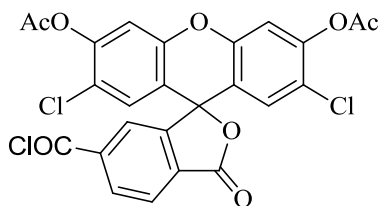
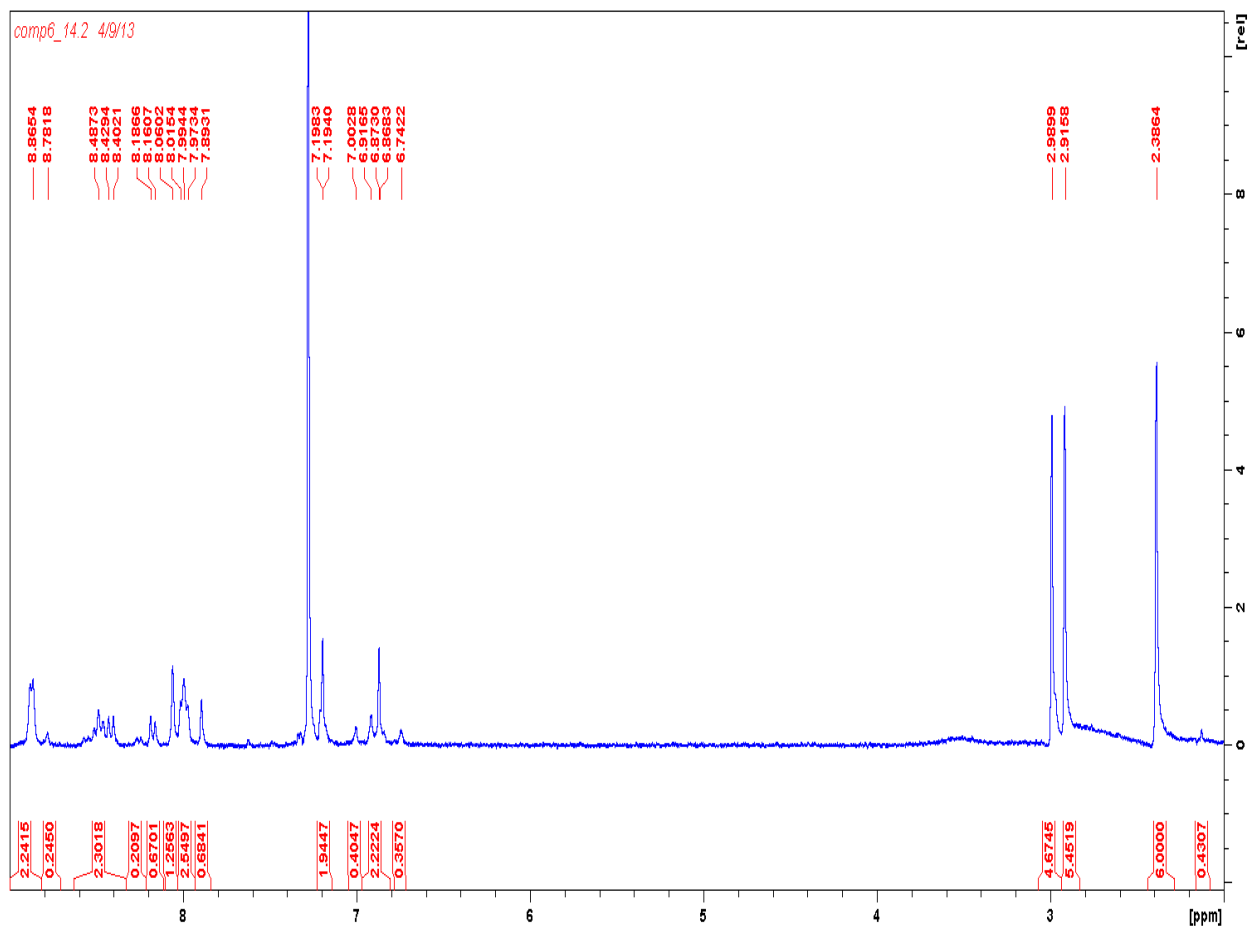


Figure 19. ^1H - NMR spectrum of compound (**6a**) in chloroform- d.

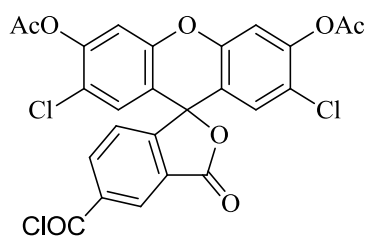
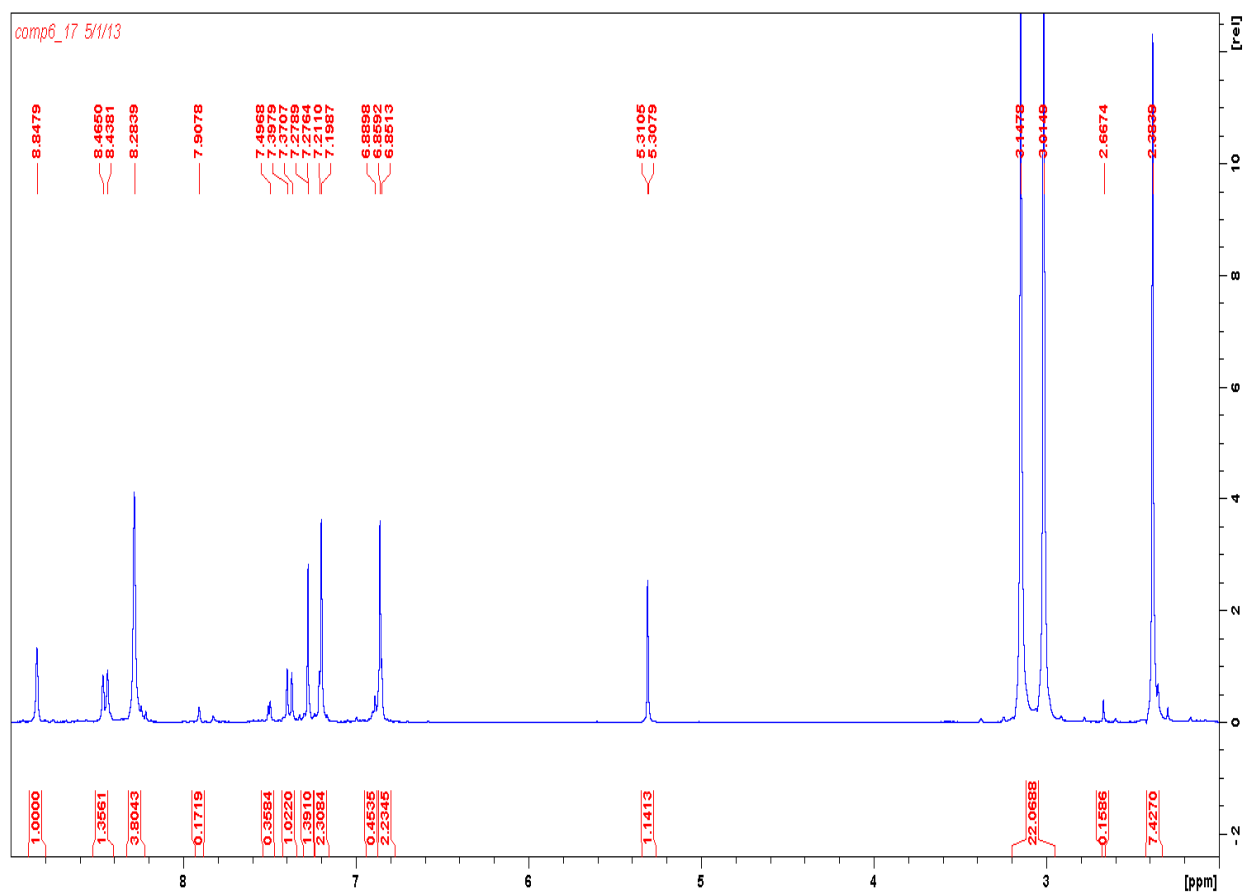


Figure 20. ^1H - NMR spectrum of compound (**6b**) in chloroform- d.

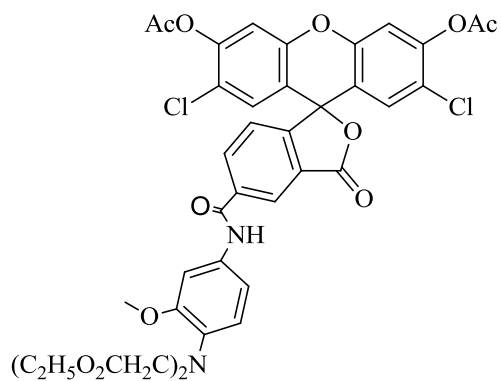
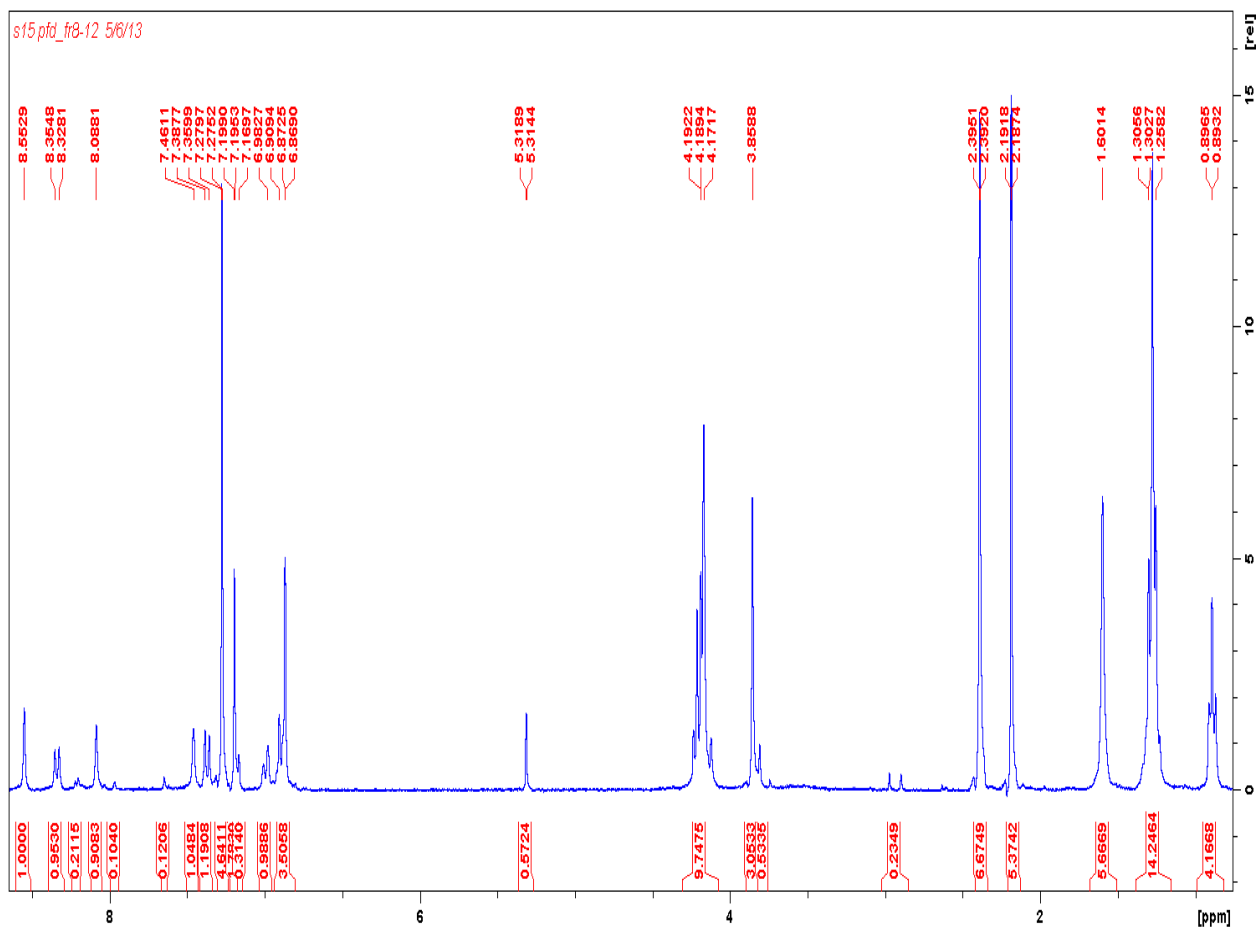


Figure 21. ¹H- NMR spectrum of desired sensor in chloroform- d.